Escola de Camins
Escola Tècnica Superior d'Enginyeria de Camins, Canals i Ports
UPC BARCELONATECH

ENVIRONMENTAL FRIENDLY MEASURES TO PROTECT THE ROMANIAN COAST

Treball realitzat per:

Monclús i Bori, Albert

Dirigit per:

Gràcia, Vicente
García-León, Manuel
Dinu, Irina

Grau en:

Enginyeria Civil

Barcelona, 20 de setembre de 2018

Departament d'Enginyeria Civil i Ambiental -DECA-

TREBALL FINAL DE GRAU

- E T S E C C P B -
Escola Tècnica Superior d'Enginyers de Camins, Canals i Ports de Barcelona

Universitat Politècnica de Catalunya

Departament d'Enginyeria Civil i Ambiental
DECA

ENVIRONMENTAL FRIENDLY MEASURES TO PROTECT THE ROMANIAN COAST

Monclús i Bori, Albert

September 20, 2018

ABSTRACT

This thesis is an initiative resulting from a national research project in collaboration with a research center in Romania -GeoEcoMar-.

Hard works (groins, detached breakwaters) induce steady hydrodynamic behaviours that can lead to local problems such as erosive gradients. These hindrances may be exacerbated at urban areas due to climate change and population pressure. Submerged vegetation -seagrass- may be a cost-effective solution for damping hydrodynamic forcings, plus alleviating some of the hard work drawbacks. The aim of this project is to evaluate the feasibility of submerged vegetation for attenuating wave energy at an urban Romanian beach, more precisely in the Mangalia-Saturn seashore. Such analysis is conducted with numerical modelling using SWAN.

The results indicate a reduction of the wave height between 8-4% in the moderate energy waves and a 3.5-2.1% in the low energy ones. This is a significant reduction of wave height and again is another evidence of its viability.

Overall, although the results are positive, grey solutions are still ahead in its performance in a more controlled and stable results. Being this green measures a feasible solution in areas where the quantity of wave height to reduce is in the order of moderate to low.

Aquest Treball de Final de Grau s'emmarca en un projecte nacional de recerca en col·laboració amb un centre d'investigació a Romania -GeoEcoMar-.

Estructures marítimes (espigons, dics exempts) indueixen comportaments hidrodinàmics regulars que poden provocar problemes locals com gradients erosius. Aquestes dificultats poden ser agreujades en àrees urbanes degut al canvi climàtic i a la pressió induïda per la població. La introducció de vegetació submergida -prades marines- poden resultar en una solució cost-efectiva per esmorteir aquestes hidrodinàmiques mentre, a la vegada, eliminen moltes de les desaventatges de la construcció d'estructures marítimes. L'objectiu d'aquest projecte es avaluar l'efectivitat de la vegetació submergida en relació a la atenuació de l'energia d'onatge en una platja rumana, concretament a la costa de Mangalia-Saturn. Aquest anàlisi s'ha realitzat utilitzant un model numèric amb el programari SWAN.

Els resultats obtinguts indiquen una reducció de l'altura d'ona d'entre un 8-4% en les onades d'energia moderada i d'un 3.5-2.1% en les onades de baixa energia. Aquesta es una significant reducció i una altra proba de la viabilitat d'aquesta green measure.

En resum, podem concloure que a pesar d'obtenir uns resultats positius, les solucions tradicionals estan encara per sobre en quan el seu rendiment donant resultats més estables i controlats. Sent aquestes green measures viables a zones on la quantitat de reducció d'altura d'ona sigui moderada-baixa.

Aceasta teza a fost realizata in urma unei colaborari cu un institut de cercetare din Romania -GeoEcoMar-.

Lucrarile de protectie costiera (epiuri, diguri sparge-val) induc modificari ale regimului hidrodinamic, care pot genera procese locale de eroziune. Astfel de fenomene pot fi accentuate in zone urbane datorita schimbarilor climatice si presiunilor antropice. Vegetatia submersa, in cazul de fata iarba de mare, poate reprezenta o solutie rentabila pentru atenuarea valurilor, fiind astfel eliminate anumite dezavantaje aferente structurilor costiere. Scopul acestui proiect este evaluarea impactului vegetatiei submerse pentru atenuarea energiei valurilor pentru o plaja urbana de pe coasta Romaniei, intre statiunile Saturn. Analiza a fost realizata prin modelare numerica, cu modelul de distributie a valurilor SWAN.

Rezultatele indica o reducere de 8-4% a valurilor de energie moderata si de 3.5-2.1% a valurilor de energie redusa. Aceasta reprezinta o reducere semnificativa a inaltimii valurilor, ceea ce arata ca solutia respectiva este viabila.

In concluzie, desi rezultatele obtinute sunt pozitive, solutiile “gri” sunt in continuare mai performante si dau rezultate mai stabile si mai usor de controlat.

Este Trabajo de Final de Grado se enmarca en un proyecto nacional de recerca en colaboración con un centro de investigación en Rumania -GeoEcoMar-.

Estructuras marítimas (espigones, diques exentos) inducen comportamientos hidrodinámicos regulares que pueden provocar problemas locales como gradientes erosivos. Estas dificultades pueden ser agravadas en áreas urbanas debido al cambio climático y a la presión inducida por la población. La introducción de vegetación sumergida -praderas marinas- puede resultar en una solución coste-efectiva para reducir estas hidrodinámicas, a la vez que eliminan muchas de las desventajas de la construcción de estructuras marítimas. El objetivo de este proyecto es evaluar la efectividad de la vegetación sumergida en relación a la atenuación de la energía de oleaje en una playa de Rumania, concretamente en la costa de Mangalia-Saturn. Este análisis se ha realizado usando un modelo numérico utilizando SWAN.

Los resultados obtenidos indican una reducción de la altura de ola de entre un 8-4% en el oleaje de energía moderada y de un 3.5-2.1% en el de baja energía. Esta es una reducción de la altura de ola significante y otra prueba de la viabilidad de esta green measure.

En resumen, podemos concluir que a pesar de obtener resultados positivos, las soluciones tradicionales están aun por encima en cuanto a rendimiento, dando resultados más estables y controlados. Siendo estas green solutions viables en lugares dónde la cantidad de reducción de la altura del oleaje sea moderada-baja.

Key words: *green measures, seagrass, submerged vegetation, Zostera noltei, wave height, wave attenuation, SWAN, Romania*

Environmental friendly measures to protect the Romanian coast

Monclús i Bori, Albert

September 20, 2018

Table of Contents

List of Figures

List of Tables

1 Introduction

1.1 Motivation

There has been an increasing preoccupation for the environment since the development of the global industrialization. But until the 90's there were no actions in order to minimize and stop this damage to the Earth. United Nations members adopted on 1st January 2016 a set of goals to encourage governments and organizations to eradicate poverty around the world and achieve a sustainable development from the economic, social and environmental perspectives. When one thinks about a sustainable environmental development the principal actions that one can think of are minimizing the burn of fuels, producing less waist in the industry, all climate change related actions, recycling, creating more efficient products, driving electric cars, etc. Nevertheless as a transversal concept it involves a lot more actions or decisions.

The decision that it has been studied on this thesis is about sea protection, analyzing if a similar result to what is obtained by constructing some structures in the sea can be achieved using green protection measures. The construction of structures in the seashore like detached breakwaters, ports, artificial reefs, etc. can produce a lot of stress to the environment. Construction works itself, sand refill, change in the sediment transport scheme, ecological harm to the coast, ecosystem alteration and many more are effects that go against the environment.

In particular, it has been studied the efficiency of wave height reduction with a field of seagrass planted near an specific place in the coast of Romania. With this information the decision-makers could evaluate the necessity of an artificial structure to protect the coast, like an artificial reef, or if it is enough to try a more green solution that will not only preserve, even improve the environmental value of the seashore as the one studied in this project.

In a more personal note, the decision of taking part of this thesis can not be explained without knowing some of my background. Since I started my studies that I am culminating now with this thesis, I have been passionate about all human made structures in the coast. Knowing more about ports, marinas and breakwaters was one of the reasons I wanted to study Civil Engineering. But I was not really aware of all collateral damage these structures can produce and how they alter the ecosystems created million years ago by the nature. Luckily some subjects like Construction Management, Environmental Engineering and Maritime and Port Engineering helped me with that, being now a more environmentally aware person. The idea of implementing the scientific concepts used for the construction of this structures to investigate and develop green measures that achieve the same objectives without any ecological challenge was very exciting. Moreover, meeting my Romanian tutor, Irina, and having the opportunity to stay some days on location -in GeoEcoMar- achieving a greater knowledge of the place and taking part of an international project was and invaluable motivator for me.

Figure 1: Foișorul de Foc, an important landmark in Bucharest near GeoEcoMar. *Source: Self-made.*

1.2 Objectives

The main objective of this thesis is to evaluate, using a numerical model, how the wave height in the coast of Mangalia-Saturn is reduced planting Zoostera Noltei seagrass in the seashore.

In order to achieve this main goal it has to be completed the next list of subtasks.

1. Defining the bathymetry of the study area and modelling it, using the data to draw it and a specific software to format, so it can be used properly in the numerical wave analysis.

2. Defining the wave climate using the data from the ECMWF -European Centre for Medium-Range Weather Forecasts- and calculating all mean wave level (without extremal cases -storms-) for each direction used.

3. Design of the wave model distribution and the vegetation mask that is going to be evaluated.

4. Using SWAN to calculate and calibrate the actual wave conditions.

5. Using SWAN to calculate how the wave conditions differ from the previous ones with the vegetation in the seashore.

6. Evaluate the difference of wave conditions in each case and the effectiveness of the use of vegetation.

1.3 Outline of the minor thesis

To first contextualize the framework of this project it has been explained the state-of-the-art. It is divided in sections according to the topic. Some of the references introduced in the topics can fall in between two or more of them, but distributing them this way is easier to find useful information if someone is interested to go deeply into only one of the topics.

The next section 'methods' explain in a very specific manner which were the steps and the overall theory of the project. It is also divided in the main three steps done in the project, ordered chronologically as they have been made. In each subsection there is explained the theory and science behind each topic and then the reproduction of what has been performed.

On the study area one explains the real environment and background of the place studied. It is not possible to extract valuable conclusions of the project without contextualizing it and getting to know which is the area of study. That is why there is a more so called big picture subsection that contextualize some general Romanian aspects, specifically related with its coast, and then there is more specific description of the studied area and its wave climate to understand the place in a physical and also more maritime related way.

The results is the most important section, where all the theory and work presented in the previous sections lead to new information and knowledge. First are presented the results extracted from the numerical model in the baseline (actual state) and vegetation (introducing numerically a vegetation mask that represents planted Zoostra Noltei) scenarios, after it there is the comparison between both cases to see more clearly the difference of wave height between them.

Having the results presented, there is a section that talks about what can be seen in them and which way they should be interpreted. This discussion leads to the next section: Conclusions. In it one can find the final thoughts and points discovered in the project.

Finally, there is a last section where is presented the next steps that should be done in order to going more in deep, have more information or develop better the idea; and tries to be a guideline for further investigation in the same direction.

2 State-of-the-art

2.1 Romanian Coast

One can find scientific literature of the Romanian coast since the early eighties. At first, and still today, the most studied part of the coast has been the Danube Delta, as it is a very important biosphere reserve for UNESCO and has a great relevance as an ecosystem of high scientific and natural interest. Examples of studies about it are Charlier and De Julio (1985), Gastescu (1983), and more recently Dan (2013).

Since the end of the Cold War and the opening of Romania to the world, that lead to the country joining the European Union in 2007, Romania experienced a high economic growth -even more during the 2000s-. This economic growth improved the living standards and people, first from Romania itself and then tourists around the world, started to go on vacation to its coast. Development of tourism also created interest for the protection and development of other coastal areas apart from the Danube Delta. This is also reflected in the scientific literature being examples of that Nenciu and Coman (1996), Panin (1996), Postolache et al. (1995), and Giosan et al. (1999).

Figure 2: Detail of the Danube Delta. *Source: NASA Earth Observatory: Where the Danube meets the Black Sea.*

When tourism became really important for the Romanian economy (Surugiu and Razvan, 2013), Romania started to put efforts in protecting it and make it more attractive for tourism. This process started with the case study in Mamaia beach -in the center of Romanian coast- in relation with the necessity of beach management (Coman et al., 1999). During this process it was also created GeoEcoMarina (1996), the research center that collaborates in this project. In 2005, was decided to realize a Coastal Protection Plan with the collaboration of the Japan International Cooperation Agency (JICA) resulting in a series of reports that were partially followed by the Romanian Government, as a large number of the recommendations and solutions (breakwater, jetties, etc.) are already constructed or have been implemented (JICA, 2007 and JICA, 2008), see Figure 3.

Figure 3: Mamaia South beach before and after the JICA Coastal Protection Plan. *Source: JICA, 2007.*

More recently another Master Plan has been realized in order to protect and rehabilitate the coastal zone (Halcrow UK, 2011-2012) plus some important studies about the reduction of coastal erosion (Halcrow Romania, 2011).

The trend now, since the publications of Halcrow seem more in line of conservation and sustainable use of the Romanian coast natural resources considering the sustainability a pillar of the development of the Romanian coastal area (Mari-Isabella, 2014).

2.2 Wave modelling

Since the democratization of computers and its capacity of quick and relivable calculation every major science have taken advantage of it. Maritime engineering is not an exception.

Before the commercialization of models for simulating waves maritime science was already using computers to calculate estimations and validate formulas and theories that already existed. But the development of a wave model was only a matter of time. In the early 1990s already existed various programs elaborated independently by different universities, but it was SWAN (Simulating WAves Nearshore) (Booij et al., 1999 and Lesser et al., 2004) the one that gain more adepts and developed furthermore. The first publication related to an old version of SWAN dates from 1993, nowadays there are more than 50 scientific publications that use SWAN as its web page points out -even it is not updated as the last publication it shows is from 2013.

But there exist more programs that are well-known and widely used as XBeach, that model morphological changes of beaches and sediment transport behaviour; BOM (Bergen Ocean Model), a three-dimensional hydrodynamic multipurpose program for coastal and shelf seas; SMS (Surface-Water Modelling System), a one, two or three-dimensional modelling program with pre- and post-processing for surface water modelling and design; and other important comercial programs.

Some references of publications that use SWAN and are related to this thesis are Blackmar et al. (2013), Bondar et al. (2001), Suzuki et al. (2012), Dinu et al. (2017) and Sierra et al. (2017).

2.3 Zostera Noltii

Zostera Noltii (Dwarf Eelgrass) is a widely studied seagrass cataloged by the IUCN Red List as a Least Concern in the Threatened Species scale. It has been studied for many years as there is no trace of when it first was named. All the specifications of the seagrass can be found in Short et al. (2010). From this paper is the Figure 4, were one can observe all the regions were one can find Zostera Noltii.

Our main interest is the possibility of transplanting a large number of specimens on location, and as Nita et al. (2014) explains, it can be done. Moreover in this scientific publication is discussed the creation of 'nurseries' to grow this specimen in controlled ecosystems to later on transplant them on location.

There are studies about the transplantation of the Zostera Noltii as its population is considered in decrease in the Black, Caspian and Aral Seas (Short et al., 2010 and Marin et al., 2013) .

Figure 4: Distribution map of Zostera Noltii segrass population. *Source: Short, F.T., et al., 2010.*

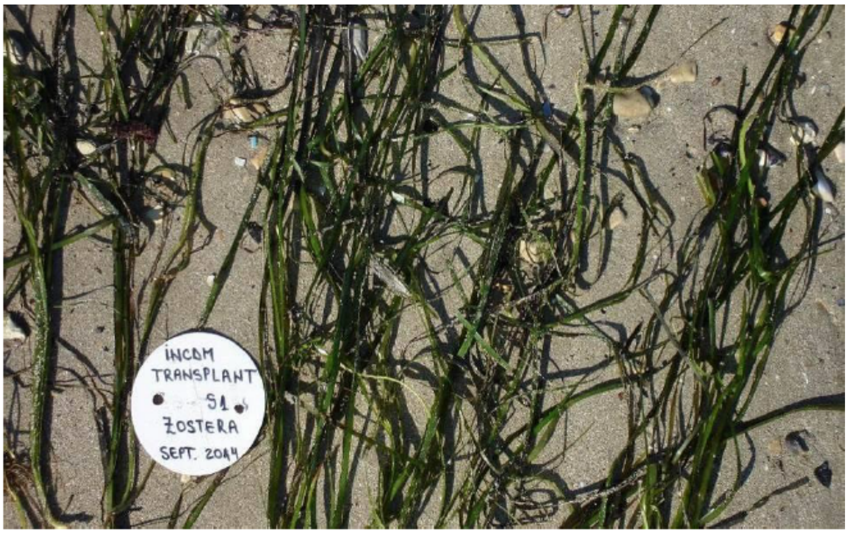

Figure 5: Zostera noltii sample and its tag before transplanting. *Source: Nita, V. et al., 2014.*

2.4 Submerged vegetation for wave attenuation

For the moment, there has not been any real application of transplanting or growing seagrass in order to minimize wave height and damp wave energy to protect a coastal zone. Nonetheless, influence of seagrass to reduce wave energy has been for a long time.

Dalrymple et al. (1984) defined what it is known as the Dalrymple's formula, which indicates Wave Diffraction due to areas of energy dissipation. This formula and this publication is the base of all this theory and it is still in use even in the computational programs as SWAN.

In 1982, Fonseca et al. (1982) published an observational study on the influence of seagrass on current flow, followed by Fonseca and Cahalan (1992) were it was evaluated various types of seagrass and salt marshes in a wave tank. On this studies it was already demonstrated the damping effect of seagrass in general -comparable to the effect of salt marshes when water depth is scaled to plant size-, the same statment can be found in Blackmar et al. (2013) and Christianen et al. (2013). In more recent studies (Koftis et al., 2013 and Manca et al., 2012) it is used Posidonia oceania (or Mediterranean tapeweed) which is a seagrass endemic o the Mediterranean Sea.

In 1993, Kobayashi et al. (1993) went one step above analysing this effect using continuity and linearized equations and comparing them with experimental tests runs. Möller et al. (1999) introduced the numerical modelling on this field of study, and also it is suggested the necessity of maintaining or even growing salt marshes as part of coastal set-back or shoreline realignment schemes.

Another important contribution in this field can be found in Möller et al. (2006), were it is found that wave attenuation by vegetation goes up to a threshold value and implies that the damping effect does not keep up for high wave heights values that can be produced, for example, in storm events. But this is not really well understood as Bouma et al. (2014) and Kirwan and Megonigal (2013) indicate. There is strong indications of vegetation causing considerable wave attenuation, even when water levels and waves are highest, but progressively flatten and break vegetation stems and thereby reduce dissipation (Möller et al., 2014) so it is not the optimal situation. It is a combined effect of stems bending and breaking progressively which reduces wave attenuation, but at the same time it still attenuates as the vegetation is lower, but denser; changing the Drag coefficient also and making its modelling more difficult.

Now more than ever before, society has deep ecological awareness. The preoccupation for the well being of The Earth and its natural resources has been increasing rapidly since the last few decades. This can also be reflected in the scientific publications of Maritime Engineering. Some examples can be Borsje et al. (2011), Narayan et al. (2016) and Pontee et al. (2016) which content relates to nature-based solutions and ecological engineering for coastal protection. Some others, as Ondivela et al. (2014), search in submerged vegetation a possible solution to mitigate the future changing climate effects to the coast, concluding that seagrass meadows cannot protect shorelines in every scenario and finding optimal conditions in shallow waters and low wave energy environments, as it was explained before.

All this studies traced, lead to the publication of Sierra et al. (2017), which projects the plantation of seagrass and assesses its effectiveness for attenuating wave energy through numerical modelling in two harbours situated in the Catalan coast. And is the major inspiration for this thesis.

3 Methods

3.1 Bathymetry

A bathymetry is the representation of the depth underwater using lines that follow the path of the soil that is at the same distance of water level. In other words, one could say that is the underwater topography. An example of a bathymetry can be seen in Figure 6.

Another important thing to understand in bathymetries in general, and more specifically in the ones near shore in any sea or ocean -like in the case study-, is that it can only aim to be a good representation of the sea floor. As it has been largely demon-

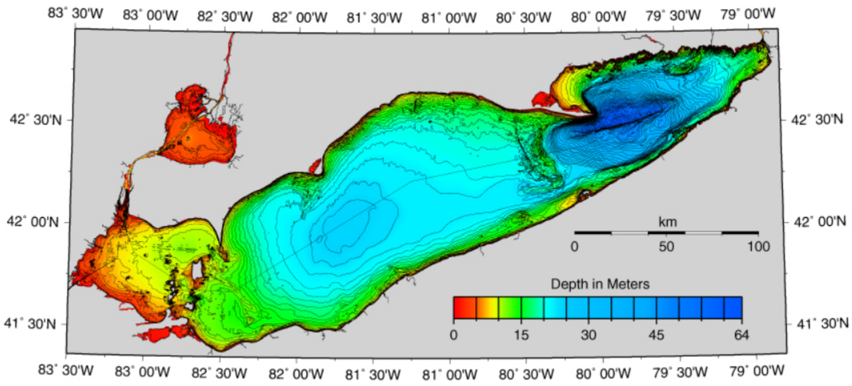

Figure 6: An example of a bathymetry, in this case of Lake Erie and Lake Saint Clair, in the Canada-USA border. *Source: National Geophysical Data Center.*

strated beach and near shore morphology varies under seasons and storm occurrences, traditionally ascribed to a variation in the incident wave energy level (Abele Jr, 1977 and Masselink and Pattiaratchi, 2001).

With the aim of having a good approximation of the soil depth in our study zone it has been collected a series of data from electronic navigational charts. Then using GIS based programs, different lines defining soil's depth are created. Those are first drown every one meter depth (until 20 m deep) and then every 2 m. It was decided to reach until 50 m depth -that only supposed a 28 km wide bathymetry-. This decision was taken for two main reasons:

- To define, for example, a 100 m depth model it required to create a bathymetry 100 km wide, as one can see at Figure 7. A model with this size would require an enormous computational cost or a rougher definition. With the scale of the zone of placement of the vegetation compared to this bigger model, the vegetation field would be represented as an only point in the numerical model. The computational costs associated were another impediment due to the limited resources that were available for this thesis.

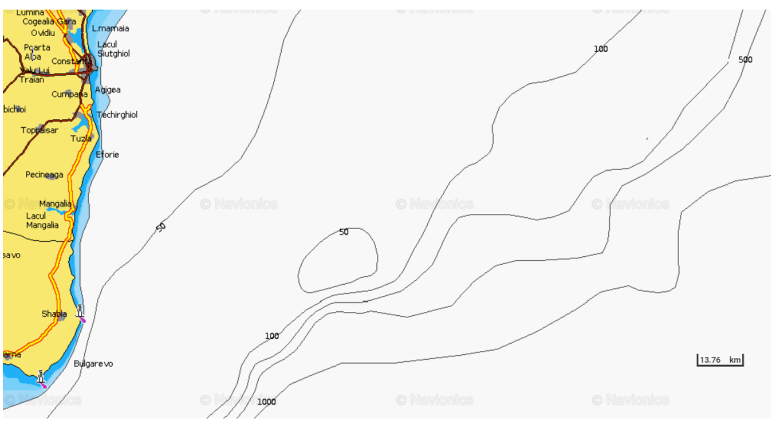

Figure 7: Bathymetry of the study area. *Source: Self-made using Navionics.*

- A possible solution for this could be proceeding with various model sizes that go from larger and rougher to smaller and more defined, as it is explained in the 3.3 section. Nevertheless with the wave conditions applied in this work, that one can see in the 3.2 section, boundary waves introduced would not experience any effect from the wave-bottom friction until 43 m deep approximately. To demonstrate this, the formula of Attenuation due to Bottom friction JONSWAP is used (Hasselmann et al., 1973). Since it is a very complex formula with a large number of parameters that is necessary to go in detail to explain it correctly, it has been decided to not go into it any further. A short sum up of its operativity can be seen in section 3.3.1.1.

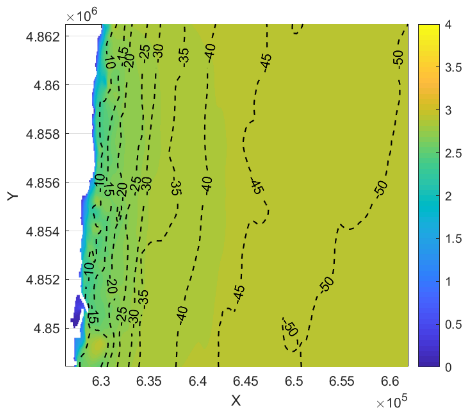

Figure 8: SWAN run using 3 m high with 10s of Tp and perpendicular to the shoreline waves. *Source: Self-made using SWAN and MATLAB.*

Instead of calculations and explanations, one can see in Figure 8 a run of SWAN using waves 3 m high with 10s of Tp (Wave period) and perpendicular direction to the shore. As SWAN uses the JONSWAP formula to calculate the attenuation due bottom friction, one can see the starting line of wave attenuation at 43 m deep approximately as it was described.

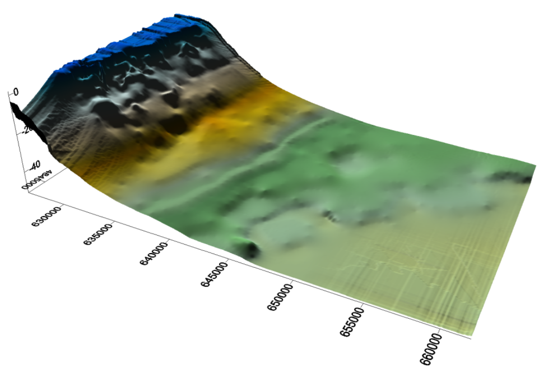

Figure 9: Representation of one of the iterations of the bathymetry with raw data, before final reshaping. *Source: Self-made using Surfer 12.*

After defining the bathymetry in the GIS program it is used a Surface creation program in order to represent the shape of the bottom of the sea in our region model, a surface crated can be seen in Figure 9. Then using Kriging as a gridding method it is calculated the grid with the specifications needed -in our case with a spacing of 80 m and 15 m in both directions x and y, trying to never exceed the 1000 nodes for bathymetry-. After this step, it is usually needed to manually change some values that not comply with reality, especially in the borders.

Finally, the last step to perform is to adapt the output grid scheme to the one that SWAN can understand in order to compute our results.

3.2 Wave Climate

The Wave Climate data used is from the ECMWF -European Centre for Medium-Range Weather Forecasts- reanalysis of 38 years wave data (Onea and Rusu, 2017). Used in Lin-Ye et al. (2017) where using SWAN and a generalized additive model it is made a hindcast and forecast of this data set. More precisely the data set used in this project is from the point 34 one can see in Figure 10. Being the data set of more than a hundred years -due to the reanalysis with hindcast and forecast performed- it was decided to only use 30 years (1988-2018).

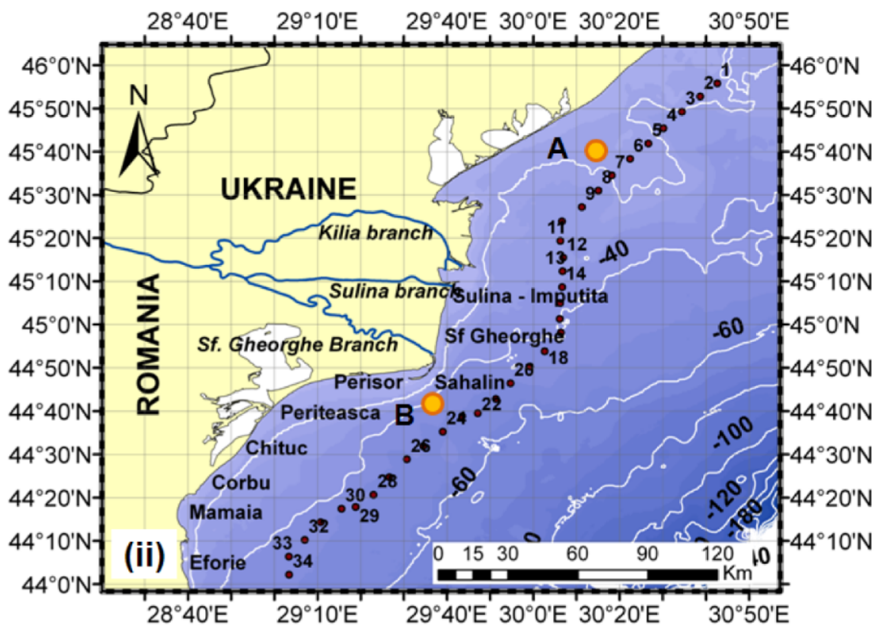

Figure 10: Nodes of the statistical model of the reanalysis in the northwestern Black Sea. The data set used in this project is from the point 34. *Source: Lin-Ye et al. (2017).*

There are two main reasons supporting the fact that only 30 years are being used:

1. The first one, and the main one, is the quantity of data. The data gives our desired three variables (Hs -wave height-, Tp -wave period- and direction -in degrees-) plus six other variables of more than a hundred years one our by one our. This is a total of more than 876000 entrances with 9 variables. The computer used had no capacity to work with this quantity of data.

2. The second reason, and the justification to use 30 years of data, is that with the

wave climate to perform this quantity of data is considered more than enough precise.

As the numerical model is about the propagation of the waves to the coast the first data to sort out are the waves that would not reach the coast, so its direction is not from 11.25° to 191.25°, see Figure 11. This range comprehends the directions NNE, NE, NEE, E, SEE, SE, SSE, S.

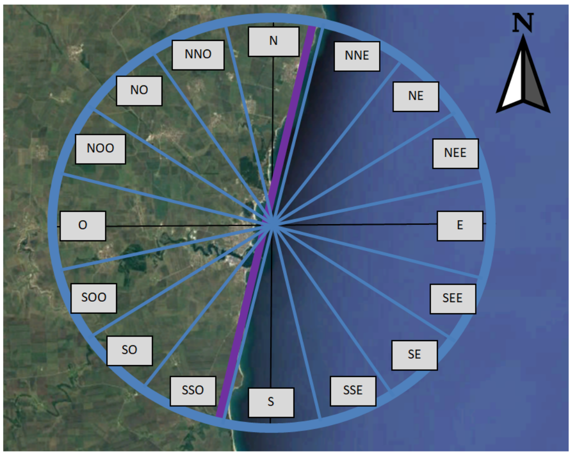

Figure 11: Layout of the coast compared with the 16 divisions -with 22.5° each- of the cardinal directions. *Source: Self-made using Google Earth.*

The next step to perform is to calculate the H_{morf} with the objective of synthesize the wave information in order to represent an average surge, it is not of our interest the extremal scenarios (or storms). The H_{morf} is defined as:

$$H_{morf} = \sqrt{\frac{\sum H_i^2 f_i}{\sum f_i}} \tag{1}$$

Where H_i is the wave height and f_i is the rate of occurrences. In order to estimate it first it has been divided the wave data in our range of directions, and then the data is classified for its wave height (in increments of 0.5 m) and wave period (in increments of 2 s). To follow with the computation of the percentage of occurrences for each case and each direction, to then obtain the H_{morf} for every period division. One can see in the tables 3, 4, 5, 6, 7, 8, 9 and 10 the percentage for each case in every direction analyzed.

The sector between 4-6 s of Tp (wave period) is the one that almost is majority in every direction (see the last row in the tables). That is the reason it is one of the columns chosen to calculate the H_{morf}. The other one is the column 8-10 s as it is the highest period with real representation in the occurrence data. This selection is made thinking on the objective that this thesis aims, as very low periods and wave heights are not really a concern for the coast protection and neither suffer from the effect of the submerged vegetation. Also are chosen a low and a moderate wave energy spectrums, so it can be analyzed in both situations.

Finally, one obtains the value of H_{morf} in every direction for this two sectors of Tp (4-6s and 8-10s); this information is summarized in the next table:

Table 1: Summarize of H_{morf} for the wave periods 4-6s and 8-10s for every direction. *Source: Self-made.*

	4 - 6 s	8 - 10 s
NNE	1.27 m	2.98 m
NE	1.15 m	3.43 m
NEE	1.06 m	2.61 m
E	0.85 m	2.33 m
SEE	1.11 m	1.79 m
SE	0.98 m	2.06 m
SSE	1.21 m	1.63 m
S	1.20 m	2.28 m

Then it was taken the decision on performing the evaluation for three of these directions. The reason is that this project tries to evaluate the feasibility of the submerged vegetation and performing all those numerical analysis would give us over information that can mislead the aim of the project. Again, the intention is to evaluate the feasibility of it, not to analyze the interactions for every direction. Also it would require a lot of time and resources, as for every case it has to be performed for the DOM1, for the DOM2 without vegetation and for the DOM2 with vegetation, see section 3.3.

The three directions chosen are: NE, E, SSE. It was a requirement to have direction distributed uniformly to verify any interesting interaction with the batyhymetry or the coast. Also as one have may seen NE has the highest wave height (in the 8-10s section) and E the lowest (in the 4-6s section), moreover SSE direction was a moderate one, having a high H_{morf} for 4-6 s and a low H_{morf} for 8-10 s compared to the other ones.

To sum up the cases (from wave climate perspective) to analyze one can see Table 2.

Table 2: Summarize of H_{morf} for the wave periods 4-6s and 8-10s for every direction. *Source: Self-made.*

NE	1.15 m	5 s
NE	3.43 m	9 s
E	0.85 m	5 s
E	2.33 m	9 s
SSE	1.21 m	5 s
SSE	1.63 m	9 s

Hs (m) \ Tp (s)	0 - 2	2 - 4	4 - 6	6 - 8	8 - 10	10 - 12	>12
0 - 0.5	0.20%	16.97%	4.11%	0.22%	0.28%	0.00%	0.00%
0.5 - 1	0.00%	17.30%	10.25%	0.94%	0.39%	0.00%	0.00%
1 - 1.5	0.00%	0.44%	18.32%	0.81%	0.07%	0.00%	0.00%
1.5 - 2	0.00%	0.00%	11.47%	0.94%	0.15%	0.00%	0.00%
2 - 2.5	0.00%	0.00%	3.50%	2.74%	0.11%	0.00%	0.00%
2.5 - 3	0.00%	0.00%	0.13%	4.27%	0.11%	0.00%	0.00%
3 - 3.5	0.00%	0.00%	0.00%	2.83%	0.02%	0.00%	0.00%
3.5 - 4	0.00%	0.00%	0.00%	1.74%	0.17%	0.00%	0.00%
4 - 4.5	0.00%	0.00%	0.00%	0.37%	0.52%	0.00%	0.00%
4.5 - 5	0.00%	0.00%	0.00%	0.07%	0.33%	0.00%	0.00%
5 - 5.5	0.00%	0.00%	0.00%	0.00%	0.11%	0.00%	0.00%
5.5 - 6	0.00%	0.00%	0.00%	0.00%	0.11%	0.00%	0.00%
6 - 6.5	0.00%	0.00%	0.00%	0.00%	0.02%	0.00%	0.00%
6.5 - 7	0.00%	0.00%	0.00%	0.00%	0.00%	0.00%	0.00%
7 - 7.5	0.00%	0.00%	0.00%	0.00%	0.00%	0.00%	0.00%
7.5 - 8	0.00%	0.00%	0.00%	0.00%	0.00%	0.00%	0.00%
8 - 8.5	0.00%	0.00%	0.00%	0.00%	0.00%	0.00%	0.00%
8.5 - 9	0.00%	0.00%	0.00%	0.00%	0.00%	0.00%	0.00%
9 - 9.5	0.00%	0.00%	0.00%	0.00%	0.00%	0.00%	0.00%
9.5 - 10	0.00%	0.00%	0.00%	0.00%	0.00%	0.00%	0.00%
>10	0.00%	0.00%	0.00%	0.00%	0.00%	0.00%	0.00%
	0.20%	34.71%	47.79%	14.91%	2.39%	0.00%	0.00%

Table 3: NNE table of occurrences (in percentage). *Self-made using MATLAB and Excel.*

Hs (m) \ Tp (s)	0 - 2	2 - 4	4 - 6	6 - 8	8 - 10	10 - 12	>12
0 - 0.5	0.18%	18.07%	7.71%	0.20%	0.16%	0.00%	0.00%
0.5 - 1	0.00%	14.04%	15.23%	0.95%	0.39%	0.00%	0.00%
1 - 1.5	0.00%	0.28%	14.77%	1.96%	0.15%	0.00%	0.00%
1.5 - 2	0.00%	0.00%	7.91%	2.85%	0.03%	0.00%	0.00%
2 - 2.5	0.00%	0.00%	1.60%	5.30%	0.07%	0.00%	0.00%
2.5 - 3	0.00%	0.00%	0.08%	3.44%	0.08%	0.00%	0.00%
3 - 3.5	0.00%	0.00%	0.00%	1.66%	0.54%	0.00%	0.00%
3.5 - 4	0.00%	0.00%	0.00%	0.54%	0.75%	0.00%	0.00%
4 - 4.5	0.00%	0.00%	0.00%	0.07%	0.47%	0.00%	0.00%
4.5 - 5	0.00%	0.00%	0.00%	0.00%	0.34%	0.00%	0.00%
5 - 5.5	0.00%	0.00%	0.00%	0.00%	0.15%	0.00%	0.00%
5.5 - 6	0.00%	0.00%	0.00%	0.00%	0.05%	0.00%	0.00%
6 - 6.5	0.00%	0.00%	0.00%	0.00%	0.00%	0.00%	0.00%
6.5 - 7	0.00%	0.00%	0.00%	0.00%	0.00%	0.00%	0.00%
7 - 7.5	0.00%	0.00%	0.00%	0.00%	0.00%	0.00%	0.00%
7.5 - 8	0.00%	0.00%	0.00%	0.00%	0.00%	0.00%	0.00%
8 - 8.5	0.00%	0.00%	0.00%	0.00%	0.00%	0.00%	0.00%
8.5 - 9	0.00%	0.00%	0.00%	0.00%	0.00%	0.00%	0.00%
9 - 9.5	0.00%	0.00%	0.00%	0.00%	0.00%	0.00%	0.00%
9.5 - 10	0.00%	0.00%	0.00%	0.00%	0.00%	0.00%	0.00%
>10	0.00%	0.00%	0.00%	0.00%	0.00%	0.00%	0.00%
	0.18%	32.38%	47.30%	16.96%	3.18%	0.00%	0.00%

Table 4: NE table of occurrences (in percentage). *Self-made using MATLAB and Excel.*

Hs (m) \ Tp (s)	0 - 2	2 - 4	4 - 6	6 - 8	8 - 10	10 - 12	>12
0 - 0.5	0.48%	22.29%	10.32%	1.08%	0.14%	0.00%	0.00%
0.5 - 1	0.00%	11.95%	16.06%	3.14%	1.39%	0.00%	0.00%
1 - 1.5	0.00%	0.29%	11.16%	2.35%	0.74%	0.00%	0.00%
1.5 - 2	0.00%	0.00%	4.12%	3.06%	0.19%	0.00%	0.00%
2 - 2.5	0.00%	0.00%	0.84%	2.82%	0.62%	0.00%	0.00%
2.5 - 3	0.00%	0.00%	0.00%	2.01%	0.67%	0.00%	0.00%
3 - 3.5	0.00%	0.00%	0.00%	0.79%	0.69%	0.00%	0.00%
3.5 - 4	0.00%	0.00%	0.00%	0.26%	1.17%	0.00%	0.00%
4 - 4.5	0.00%	0.00%	0.00%	0.07%	0.74%	0.00%	0.00%
4.5 - 5	0.00%	0.00%	0.00%	0.00%	0.43%	0.00%	0.00%
5 - 5.5	0.00%	0.00%	0.00%	0.00%	0.10%	0.00%	0.00%
5.5 - 6	0.00%	0.00%	0.00%	0.00%	0.02%	0.00%	0.00%
6 - 6.5	0.00%	0.00%	0.00%	0.00%	0.00%	0.00%	0.00%
6.5 - 7	0.00%	0.00%	0.00%	0.00%	0.00%	0.00%	0.00%
7 - 7.5	0.00%	0.00%	0.00%	0.00%	0.00%	0.00%	0.00%
7.5 - 8	0.00%	0.00%	0.00%	0.00%	0.00%	0.00%	0.00%
8 - 8.5	0.00%	0.00%	0.00%	0.00%	0.00%	0.00%	0.00%
8.5 - 9	0.00%	0.00%	0.00%	0.00%	0.00%	0.00%	0.00%
9 - 9.5	0.00%	0.00%	0.00%	0.00%	0.00%	0.00%	0.00%
9.5 - 10	0.00%	0.00%	0.00%	0.00%	0.00%	0.00%	0.00%
>10	0.00%	0.00%	0.00%	0.00%	0.00%	0.00%	0.00%
	0.48%	34.52%	42.49%	15.59%	6.92%	0.00%	0.00%

Table 5: NEE table of occurrences (in percentage). *Self-made using MATLAB and Excel.*

Hs (m) \ Tp (s)	0 - 2	2 - 4	4 - 6	6 - 8	8 - 10	10 - 12	>12
0 - 0.5	0.43%	17.05%	10.60%	1.76%	0.37%	0.00%	0.00%
0.5 - 1	0.00%	10.47%	16.82%	10.10%	2.33%	0.00%	0.00%
1 - 1.5	0.00%	0.07%	6.65%	6.48%	1.73%	0.00%	0.00%
1.5 - 2	0.00%	0.00%	2.96%	3.42%	1.50%	0.00%	0.00%
2 - 2.5	0.00%	0.00%	0.37%	2.06%	0.83%	0.00%	0.00%
2.5 - 3	0.00%	0.00%	0.00%	1.03%	0.90%	0.00%	0.00%
3 - 3.5	0.00%	0.00%	0.00%	0.27%	0.53%	0.00%	0.00%
3.5 - 4	0.00%	0.00%	0.00%	0.00%	0.83%	0.00%	0.00%
4 - 4.5	0.00%	0.00%	0.00%	0.00%	0.20%	0.00%	0.00%
4.5 - 5	0.00%	0.00%	0.00%	0.00%	0.13%	0.00%	0.00%
5 - 5.5	0.00%	0.00%	0.00%	0.00%	0.10%	0.00%	0.00%
5.5 - 6	0.00%	0.00%	0.00%	0.00%	0.03%	0.00%	0.00%
6 - 6.5	0.00%	0.00%	0.00%	0.00%	0.00%	0.00%	0.00%
6.5 - 7	0.00%	0.00%	0.00%	0.00%	0.00%	0.00%	0.00%
7 - 7.5	0.00%	0.00%	0.00%	0.00%	0.00%	0.00%	0.00%
7.5 - 8	0.00%	0.00%	0.00%	0.00%	0.00%	0.00%	0.00%
8 - 8.5	0.00%	0.00%	0.00%	0.00%	0.00%	0.00%	0.00%
8.5 - 9	0.00%	0.00%	0.00%	0.00%	0.00%	0.00%	0.00%
9 - 9.5	0.00%	0.00%	0.00%	0.00%	0.00%	0.00%	0.00%
9.5 - 10	0.00%	0.00%	0.00%	0.00%	0.00%	0.00%	0.00%
>10	0.00%	0.00%	0.00%	0.00%	0.00%	0.00%	0.00%
	0.43%	27.58%	37.39%	25.12%	9.47%	0.00%	0.00%

Table 6: E table of occurrences (in percentage). *Self-made using MATLAB and Excel.*

Hs (m) \ Tp (s)	0 - 2	2 - 4	4 - 6	6 - 8	8 - 10	10 - 12	>12
0 - 0.5	0.71%	21.76%	11.49%	1.15%	0.39%	0.00%	0.00%
0.5 - 1	0.00%	10.31%	17.42%	7.78%	1.03%	0.00%	0.00%
1 - 1.5	0.00%	0.20%	7.66%	6.56%	1.34%	0.00%	0.00%
1.5 - 2	0.00%	0.00%	1.97%	3.59%	0.91%	0.00%	0.00%
2 - 2.5	0.00%	0.00%	0.24%	1.86%	0.91%	0.00%	0.00%
2.5 - 3	0.00%	0.00%	0.04%	0.91%	0.71%	0.00%	0.00%
3 - 3.5	0.00%	0.00%	0.00%	0.08%	0.36%	0.00%	0.00%
3.5 - 4	0.00%	0.00%	0.00%	0.04%	0.43%	0.00%	0.00%
4 - 4.5	0.00%	0.00%	0.00%	0.00%	0.12%	0.00%	0.00%
4.5 - 5	0.00%	0.00%	0.00%	0.00%	0.04%	0.00%	0.00%
5 - 5.5	0.00%	0.00%	0.00%	0.00%	0.00%	0.00%	0.00%
5.5 - 6	0.00%	0.00%	0.00%	0.00%	0.00%	0.00%	0.00%
6 - 6.5	0.00%	0.00%	0.00%	0.00%	0.00%	0.00%	0.00%
6.5 - 7	0.00%	0.00%	0.00%	0.00%	0.00%	0.00%	0.00%
7 - 7.5	0.00%	0.00%	0.00%	0.00%	0.00%	0.00%	0.00%
7.5 - 8	0.00%	0.00%	0.00%	0.00%	0.00%	0.00%	0.00%
8 - 8.5	0.00%	0.00%	0.00%	0.00%	0.00%	0.00%	0.00%
8.5 - 9	0.00%	0.00%	0.00%	0.00%	0.00%	0.00%	0.00%
9 - 9.5	0.00%	0.00%	0.00%	0.00%	0.00%	0.00%	0.00%
9.5 - 10	0.00%	0.00%	0.00%	0.00%	0.00%	0.00%	0.00%
>10	0.00%	0.00%	0.00%	0.00%	0.00%	0.00%	0.00%
	0.71%	32.27%	38.82%	21.96%	6.24%	0.00%	0.00%

Table 7: SEE table of occurrences (in percentage). *Self-made using MATLAB and Excel.*

Hs (m) \ Tp (s)	0 - 2	2 - 4	4 - 6	6 - 8	8 - 10	10 - 12	>12
0 - 0.5	1.06%	35.07%	7.98%	2.18%	0.48%	0.00%	0.00%
0.5 - 1	0.00%	17.56%	13.15%	3.67%	1.17%	0.00%	0.00%
1 - 1.5	0.00%	0.59%	7.29%	2.08%	0.69%	0.00%	0.00%
1.5 - 2	0.00%	0.00%	2.98%	0.90%	0.16%	0.00%	0.00%
2 - 2.5	0.00%	0.00%	0.53%	0.53%	0.59%	0.00%	0.00%
2.5 - 3	0.00%	0.00%	0.11%	0.37%	0.32%	0.00%	0.00%
3 - 3.5	0.00%	0.00%	0.00%	0.11%	0.11%	0.00%	0.00%
3.5 - 4	0.00%	0.00%	0.00%	0.05%	0.05%	0.00%	0.00%
4 - 4.5	0.00%	0.00%	0.00%	0.05%	0.05%	0.00%	0.00%
4.5 - 5	0.00%	0.00%	0.00%	0.00%	0.00%	0.00%	0.00%
5 - 5.5	0.00%	0.00%	0.00%	0.00%	0.11%	0.00%	0.00%
5.5 - 6	0.00%	0.00%	0.00%	0.00%	0.00%	0.00%	0.00%
6 - 6.5	0.00%	0.00%	0.00%	0.00%	0.00%	0.00%	0.00%
6.5 - 7	0.00%	0.00%	0.00%	0.00%	0.00%	0.00%	0.00%
7 - 7.5	0.00%	0.00%	0.00%	0.00%	0.00%	0.00%	0.00%
7.5 - 8	0.00%	0.00%	0.00%	0.00%	0.00%	0.00%	0.00%
8 - 8.5	0.00%	0.00%	0.00%	0.00%	0.00%	0.00%	0.00%
8.5 - 9	0.00%	0.00%	0.00%	0.00%	0.00%	0.00%	0.00%
9 - 9.5	0.00%	0.00%	0.00%	0.00%	0.00%	0.00%	0.00%
9.5 - 10	0.00%	0.00%	0.00%	0.00%	0.00%	0.00%	0.00%
>10	0.00%	0.00%	0.00%	0.00%	0.00%	0.00%	0.00%
	1.06%	53.22%	32.04%	9.95%	3.73%	0.00%	0.00%

Table 8: SE table of occurrences (in percentage). *Self-made using MATLAB and Excel.*

Hs (m) \ Tp (s)	0 - 2	2 - 4	4 - 6	6 - 8	8 - 10	10 - 12	>12
0 - 0.5	1.03%	34.23%	4.80%	0.49%	0.22%	0.00%	0.00%
0.5 - 1	0.00%	24.45%	11.08%	1.79%	0.99%	0.00%	0.00%
1 - 1.5	0.00%	0.67%	9.74%	1.39%	0.27%	0.00%	0.00%
1.5 - 2	0.00%	0.00%	3.68%	0.72%	0.31%	0.00%	0.00%
2 - 2.5	0.00%	0.00%	1.21%	0.81%	0.13%	0.00%	0.00%
2.5 - 3	0.00%	0.00%	0.09%	0.94%	0.09%	0.00%	0.00%
3 - 3.5	0.00%	0.00%	0.00%	0.45%	0.04%	0.00%	0.00%
3.5 - 4	0.00%	0.00%	0.00%	0.13%	0.00%	0.00%	0.00%
4 - 4.5	0.00%	0.00%	0.00%	0.09%	0.13%	0.00%	0.00%
4.5 - 5	0.00%	0.00%	0.00%	0.00%	0.00%	0.00%	0.00%
5 - 5.5	0.00%	0.00%	0.00%	0.00%	0.00%	0.00%	0.00%
5.5 - 6	0.00%	0.00%	0.00%	0.00%	0.00%	0.00%	0.00%
6 - 6.5	0.00%	0.00%	0.00%	0.00%	0.00%	0.00%	0.00%
6.5 - 7	0.00%	0.00%	0.00%	0.00%	0.00%	0.00%	0.00%
7 - 7.5	0.00%	0.00%	0.00%	0.00%	0.00%	0.00%	0.00%
7.5 - 8	0.00%	0.00%	0.00%	0.00%	0.00%	0.00%	0.00%
8 - 8.5	0.00%	0.00%	0.00%	0.00%	0.00%	0.00%	0.00%
8.5 - 9	0.00%	0.00%	0.00%	0.00%	0.00%	0.00%	0.00%
9 - 9.5	0.00%	0.00%	0.00%	0.00%	0.00%	0.00%	0.00%
9.5 - 10	0.00%	0.00%	0.00%	0.00%	0.00%	0.00%	0.00%
>10	0.00%	0.00%	0.00%	0.00%	0.00%	0.00%	0.00%
	1.03%	59.35%	30.60%	6.82%	2.20%	0.00%	0.00%

Table 9: SSE table of occurrences (in percentage). *Self-made using MATLAB and Excel.*

Hs (m) \ Tp (s)	0 - 2	2 - 4	4 - 6	6 - 8	8 - 10	10 - 12	>12
0 - 0.5	0.74%	20.43%	3.39%	0.40%	0.12%	0.00%	0.00%
0.5 - 1	0.00%	21.83%	11.45%	1.26%	0.32%	0.00%	0.00%
1 - 1.5	0.00%	0.48%	14.94%	2.35%	0.20%	0.00%	0.00%
1.5 - 2	0.00%	0.00%	7.36%	2.37%	0.28%	0.00%	0.00%
2 - 2.5	0.00%	0.00%	2.23%	3.95%	0.32%	0.00%	0.00%
2.5 - 3	0.00%	0.00%	0.02%	2.73%	0.28%	0.00%	0.00%
3 - 3.5	0.00%	0.00%	0.00%	1.46%	0.24%	0.00%	0.00%
3.5 - 4	0.00%	0.00%	0.00%	0.28%	0.24%	0.00%	0.00%
4 - 4.5	0.00%	0.00%	0.00%	0.04%	0.20%	0.00%	0.00%
4.5 - 5	0.00%	0.00%	0.00%	0.00%	0.04%	0.00%	0.00%
5 - 5.5	0.00%	0.00%	0.00%	0.00%	0.02%	0.00%	0.00%
5.5 - 6	0.00%	0.00%	0.00%	0.00%	0.04%	0.00%	0.00%
6 - 6.5	0.00%	0.00%	0.00%	0.00%	0.00%	0.00%	0.00%
6.5 - 7	0.00%	0.00%	0.00%	0.00%	0.00%	0.00%	0.00%
7 - 7.5	0.00%	0.00%	0.00%	0.00%	0.00%	0.00%	0.00%
7.5 - 8	0.00%	0.00%	0.00%	0.00%	0.00%	0.00%	0.00%
8 - 8.5	0.00%	0.00%	0.00%	0.00%	0.00%	0.00%	0.00%
8.5 - 9	0.00%	0.00%	0.00%	0.00%	0.00%	0.00%	0.00%
9 - 9.5	0.00%	0.00%	0.00%	0.00%	0.00%	0.00%	0.00%
9.5 - 10	0.00%	0.00%	0.00%	0.00%	0.00%	0.00%	0.00%
>10	0.00%	0.00%	0.00%	0.00%	0.00%	0.00%	0.00%
	0.74%	42.74%	39.37%	14.84%	2.31%	0.00%	0.00%

Table 10: S table of occurrences (in percentage). *Self-made using MATLAB and Excel.*

3.3 SWAN model

To perform this analysis one have to take into account the actual state of the wave propagation to then compare it with the vegetation scenario. This is the reason it can be seen a Baseline Scenario and a Vegetation Scenario for each direction evaluated in the results section. This only meant to evaluate with and without vegetation our model.

In order to proceed evaluating wave height attenuation due to submerged vegetation it is required to propagate the waves from deep waters until shallow waters, where the seagrass field is situated. Having a detailed mesh, large enough to cover all this space, was not feasible as it would have required enormous computational costs and it was not really necessary, instead it was a better option to use nesting. In this case nesting means to define two different domains with different sizes being the smaller one (DOM2) finer than the larger one (DOM1). In Figure 12 one can see DOM1 and DOM2 in the same image, as well as the seagrass field.

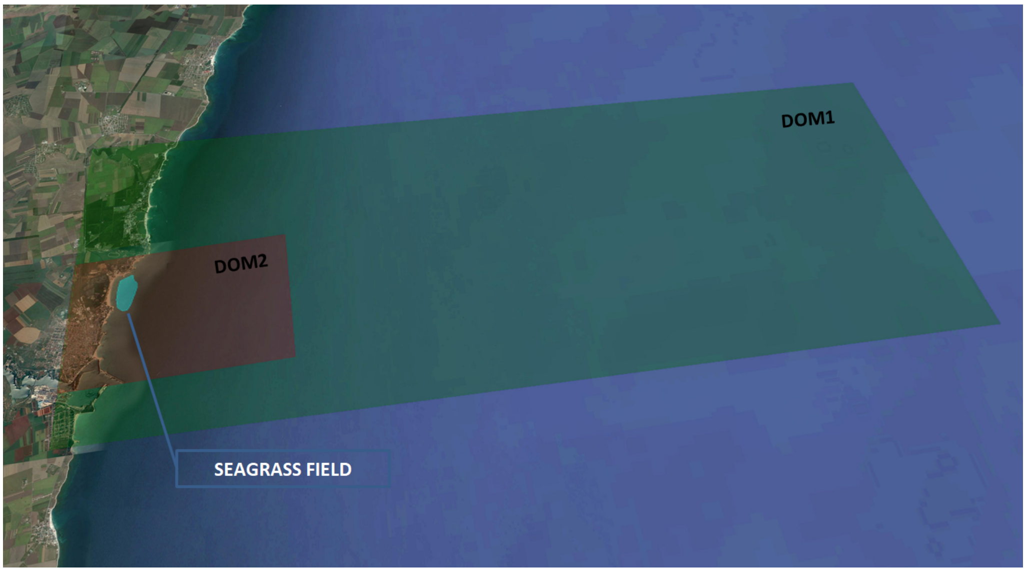

Figure 12: Representation of the two domains of the nesting. *Source: Self-made using Google Earth.*

The configuration of the domains are based on a regular mesh -there is no curvilinear mesh in this project as it has not been necessary- with a grid spacing equal in both directions (Δx and Δy). The spacing in DOM1 is 80 m and in DOM1 15 m. The perimeter and square distances of DOM1 are 97.3 km and 476 km^2, and for DOM2 are 28.6 km and 49 km^2. A table that sum up this information can be seen in Table 11.

Table 11: Type of mesh and grid spacing sizes in DOM1 and DOM2. *Source: Self-made.*

	Type	Δx	Δy
DOM1	Regular	80 m	80 m
DOM2	Regular	15 m	15 m

The process of nesting between both domains and in both scenarios is:

1. The starting point is aimed to obtain wave data required in the input of boundary conditions, explained and shown in 3.2 sector.

2. Then the Baseline Scenarios propagation/modelization are conducted in our first domain (DOM1) for all directions (from NEE to S) with this boundary conditions.

3. Then it is stored the data computed that surround the second domain (DOM2) for every direction.

4. Now, the stored data can be used as the new boundary conditions to propagate the Baseline Scenario's in the DOM2.

5. Using the same previous data stored as boundary conditions, the Vegetation Scenario is propagated in the DOM2 for all directions considered.[1]

Figure 13 can help to visualize these steps explained above using nesting. Thanks to the nesting it is solved the problem of unreasonable computation costs maintaining or even improving the model accuracy.

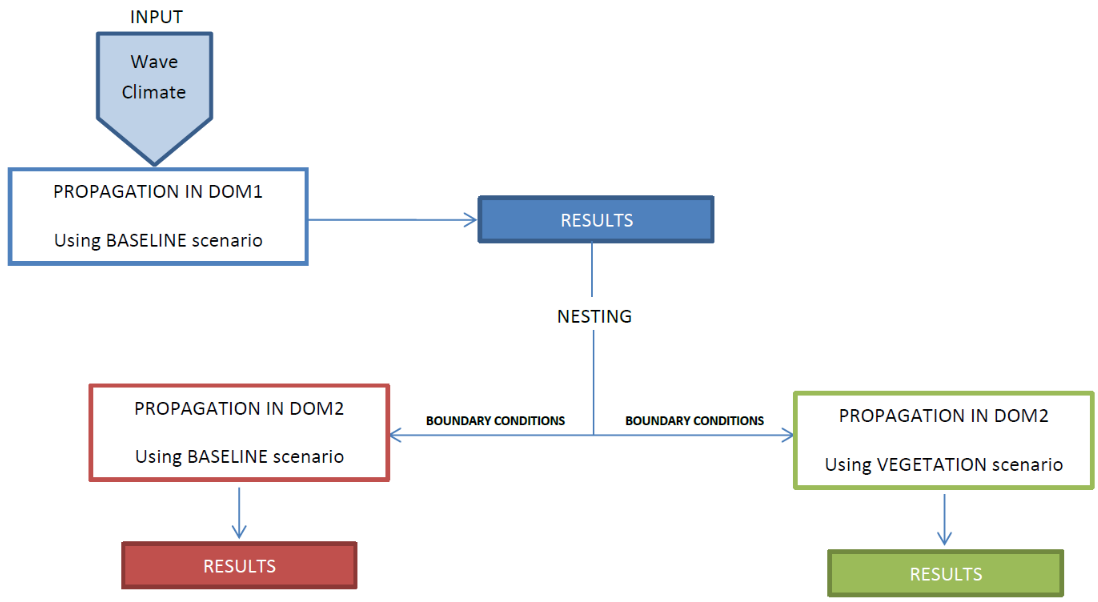

Figure 13: General outline of the nesting performed in the project. *Source: Self-made.*

In Booij et al. (1999) it is concluded that SWAN obtains acceptable results using this nesting system if it was adequatly performed. In this project are followed the basic recommendations given.

[1]Notice that the Vegetation Scenario is not modelled in the first domain (DOM1), this is because being it a so poor detailed model the vegetation had no effect on the propagation.

3.3.1 Wave model - SWAN theory

This subsection related to the theory of SWAN is an adaptation of Grases (2017) and Castell (2018) which are at the same time an adaptation of the SWAN scientific and technical documentation (The SWAN team, 2018), SWAN main article (Booij, 1999) and a textbook written by one of SWAN's developers (Holthuijsen, 2007).

"SWAN (Simulating WAves Nearshore) is a third generation, phased-averaged, open source numerical model based on the so called "action-balance equation". There are two main fields of knowledge that build up SWAN theoretical basis:

1. The description of the waves to propagate obtained from statistics obtained through observations -and in our case observations plus hindcast-: this is the random-phase/amplitude model.

2. The generation, propagation and dissipation of the waves: using the linear wave theory -also called Airy wave theory (Airy, 1841)-.

The spectral energy balance equation, which describes the evolution of the energy density spectrum, is the consequence of the combination of this two ideas. This energy density spectrum has been defined through the random-phase/amplitude model and following the linear wave theory.

Since natural phenomena are very complex, both theories were developed under some hyphothesis that limit their applicability when non-linear processes are strong, which happens in very shallow water.

In these cases non-linear models, based on the Boussinesq equations, for instance, could be used. However, as Holthuijsen (2007) points out, they have a very high computational cost that limits their application to small areas, which makes them not suitable for day-to-day practice in engineering.

Fortunately, spectral energy balance models can be extended to shallow water implementing some corrections to account for those phenomena that occur when waves approach to the coastline (refraction, shoaling, diffraction, etc.) achieving quite good estimations of the significant wave height, period and mean wave direction (Holthuijsen, 2007).

The random-phase/amplitude model

The random-phase/amplitude model postulates that the sea surface elevation, at any location and time, can be reproduced by a large sum of harmonic wave components:

$$\underline{\eta}(t) = \sum_{n=1}^{N} \underline{a}_i \cos w_i t + \underline{\varphi}_i \tag{2}$$

Where a_i is the wave amplitude, φ_i is the wave phase and w_i is the radian frequency. The underscore indicates that $\underline{a}_i$ and $\underline{\varphi}_i$ are random variables, since two statistically identical events (e.g. two storms with the same characteristics) will lead at the same point to similar but not identical values of the sea surface elevation.

Those random variables are described through density probability functions. For each wave frequency f_i, wave amplitude a_i, is considered to be Rayleigh distributed and wave phase $\underline{\varphi}_i$, is assumed uniformly distributed (phase values are equally probable between 0 and 2π.

The main hypothesis of the random-phase/amplitude model is the definition of the sea surface as stationary -when equilibrium is reached wave characteristics can be considered independent of time-. To relate this model with real observations wave records have to be of a limited duration (15-30 minutes), in which sea conditions are almost stationary. Besides, it is assumed that each wave component has been generated and has travelled independently from each other. According to the central limit theorem, the sum of a large number of independent random variables is Gaussian (or normal) distributed. This is mostly true for open ocean conditions but not in shallow waters, where steep or high waves do interact.

The energy density spectrum provides with a complete statistical and physical description of the sea surface elevation, from which ocean waves can be characterized given that random-phase/amplitude model hypothesis are fulfilled. Figure 14 flow diagram shows in a simplified manner how it is derived.

Linear Wave Theory

Linear wave theory is based on two key equations, the mass balance equation and the momentum balance equation, and a series of hypothesis:

1. The amplitude of waves must be small compared with its wave length and water depth. This condition is fairly satisfied in deep waters but not in shallow waters, where waves are steeper and water depth is small.

2. Water is assumed to be an ideal fluid: incompressible, with constant density and with no viscosity. Density can be considered constant over small regions because sea density gradients (in time and space) are small. However, in case of river discharge, vertical density variations can be important.

3. Water must be continuous, which means that there is no presence of air bubbles. Obviously, this condition is not accomplished at the surf zone, where waves break.

4. Hypothesis on boundary conditions:

   (a) Kinematic BC: related to the motion of water particles. Particles may not leave the water surface; this is condition is also violated at the surf zone. Particles may not penetrate the bottom (bottom must be infinitely rigid and dense, i.e. no porous or moving bottom is admitted).

   (b) Dynamic BC: related to the forces acting on the water particles. The atmospheric pressure at the water surface is constant (free waves, i.e. no wind pressure. Wave generation by wind is treated separately). Waves are only subjected to gravitational forces; in addition to wind forcing, surface tension and Coriolis forces are not considered in the linear theory, which limits the admissible wave length range (very small or very large waves could not be modelled).

Three-dimensional variation of the sea surface elevation

Propagation of the harmonic wave in the x-y space, in direction θ relative to the x-axis.

$$\underline{\eta}(x, y, t) = \sum_{i=1}^{N}\sum_{j=1}^{M} \underline{a}_{i,j} \cos(w_i t - k_i x \cos\theta_j - k_i y \sin\theta_j + \underline{\alpha}_{i,j})$$

Where k_i is the wave number, $k_i = 2\pi/L_i$, being L_i the wave length. Radian frequency and wave number are uniquely related according to the linear wave theory of infra-gravity waves:

$$w_i{}^2 = g k_i \tanh k_i d$$

Where d is the water depth.

Variance spectrum

Average of the squared surface elevation relative to its mean.

$$E\left(\underline{\eta_i}^2\right) = E\left(\frac{1}{2}\underline{a_i}^2\right) \; [m^2]$$

Being a_i the amplitude associated to frequency f_i.

Variance density spectrum

Distribution of the variance over frequencies and directions.

$$E_{variance}(f, \theta) = \lim_{\Delta f \to 0} \lim_{\Delta\vartheta \to 0} \frac{1}{\Delta f}\frac{1}{\Delta\theta} E\left(\frac{1}{2}\underline{a}^2\right) \left[\frac{m^2/Hz}{radian}\right]$$

No subscripts are used since this spectrum is continuous (frequency and direction intervals tend to zero).

Energy density spectrum

The energy of a harmonic wave per unit of horizontal surface area can be expressed as the product of the sea surface mean square elevation by the density of water and the gravitational acceleration.

$$Total\ energy = \rho g \sum_{i=1}^{N} \underline{\eta_i}^2 \; [J/m^2]$$

Therefore, the energy density spectrum is:

$$E_{energy}(f, \theta) = \rho g E_{variance}(f, \theta)$$

This spectrum distributes the wave energy over frequencies and propagation directions.

Figure 14: Determination of the energy density spectrum according to the random-phase/amplitude model. *Source: Grases, 2017 from Booij, 1999; Holthuijsen, 2007 and The SWAN team, 2018).*

The mass balance equation per unit volume is the following:

$$\frac{\partial \rho}{\partial t} + \frac{\partial \rho u_x}{\partial x} + \frac{\partial \rho u_y}{\partial y} + \frac{\partial \rho u_z}{\partial z} = S_p \tag{3}$$

Considering that no local generation or disappearance of water mass is produced and applying the hypothesis that states that water density is constant, the mass balance equation can be rewritten into the continuity equation, where water density no longer plays a role:

$$\frac{\partial \rho u_x}{\partial x} + \frac{\partial \rho u_y}{\partial y} + \frac{\partial \rho u_z}{\partial z} = 0 \tag{4}$$

On the other hand, the momentum balance equation is obtained from the definition of the momentum density of water, which is the product of the mass density of water and the velocity of water particles:

$$\rho \overrightarrow{u} = \{\rho u_x, \rho u_y, \rho u_z\} \tag{5}$$

The momentum balance equation for the x-component per unit volume is displayed below (5), were the source term is identified as an external force acting on the water body, so the momentum density of water is interpreted as a stress flowing through the water body.

$$\frac{\partial (\rho u_x)}{\partial t} + \frac{\partial u_x(\rho u_x)}{\partial x} + \frac{\partial u_y(\rho u_x)}{\partial y} + \frac{\partial u_z(\rho u_x)}{\partial z} = S_p = F_x \tag{6}$$

Retaining only the linear terms of the equation, considering that the external forcing is due solely to the pressure gradient and taking into account that mass density is constant, the previous expression for the x, y and z direction are reduced to:

$$\frac{\partial u_x}{\partial t} = -\frac{1}{\rho}\frac{\partial p}{\partial x} \tag{7}$$

$$\frac{\partial u_y}{\partial t} = -\frac{1}{\rho}\frac{\partial p}{\partial y} \tag{8}$$

$$\frac{\partial u_z}{\partial t} = -\frac{1}{\rho}\frac{\partial p}{\partial z} - g \tag{9}$$

As it can be seen, the self-weight of water volume ($\rho g \Delta V$) has been added to the momentum balance equation in the z-direction (8). Both mass and momentum balance equations are then expressed in terms of the so called velocity potential function:

$$\Phi = \Phi(x, y, z, t) \tag{10}$$

such that

$$\nabla \Phi = \overrightarrow{u} = \{u_x; u_y; u_z\} = \{\frac{\partial \Phi}{\partial x}; \frac{\partial \Phi}{\partial y}; \frac{\partial \Phi}{\partial z}\} \tag{11}$$

This function has no clear physical meaning, it is used just to simplify the analytical solution of the balance equations. Using the velocity potential function, the continuity equation is transformed into the Laplace equation, whose analytical solution subject to the kinematic boundary conditions provides the expression of the velocity potential function, which allows to deduce water particles' velocity equations. On the other hand, substituting water particle velocities by the velocity potential function into the momentum balance equation results in the linearized Bernoulli equation for unsteady flow. Taking into account the dynamic boundary conditions and the expression of the velocity potential function obtained from the solution of the Laplace equation, the wave-induced pressure can be derived. Finally, from all these previous results the wave energy flux expression is obtained, which relates the linear wave theory with the random-phase amplitude model. This explanation is summarized in Figure 15.

The energy balance equation

The objective of the SWAN model is to predict the energy density spectrum at any point of the study domain given a certain boundary conditions since it provides a complete description of the sea surface elevation. This is done performing a local energy density balance at several points of the domain at the same time until a stationary situation is reached.

In other words, a grid pattern is drawn over the study region and the energy density spectrum is computed at each node of the grid for each time step until the solution converges. This way of solving the problem is called the Eulerian approach ("the observer position is fixed and watches the fluid motion in different locations").

Considering a grid cell with size Δx in the x-direction and Δy in the y-direction, the energy balance equation can be expressed as follows:

$$\frac{\partial E}{\partial t} = -\frac{\partial c_g, xE}{\partial x} - \frac{\partial c_g, yE}{\partial y} - \frac{\partial c_\theta E}{\partial \vartheta} + S \tag{12}$$

Where the first term represents the change of energy density in the cell, the second and third represent the net import of energy density due to unidirectional propagation, the fourth term represents the net imporrt of energy density due to refraction and diffraction induced wave turning and the fifth term represent the local generation/dissipation of energy density.

The action balance equation

In the presence of an ambient current[2] wave energy transport is modified. Firstly, there exists an energy transference between the wave and the current. Secondly, due to the presence of the current wave propagation is modified (three phenomena occur: refraction, energy bunching and frequency-shifting).

One important term to define the action balance equation is the relative frequency σ. When a wave that propagates over a current is observed from a fixed reference system (e.g. at the seabed), the widely known Doppler effect occurs: there is a bunching of the wave crests and troughs at the front of the wave while they separate at the back of the wave (this is supposing that both wave and current travel in the same direction).

However, if the reference system moves at the same velocity than the current no Doppler effect is observed. The frequency of the wave in this situation is called relative

[2]Ambient currents are caused by oceanic scale phenomena (wind, water density gradients, Coriolis effect), tides or by wave interaction with the shoreline (rip currents due to wave breaking, long-shore currents caused by oblique incidence of the waves with respect to the shoreline).

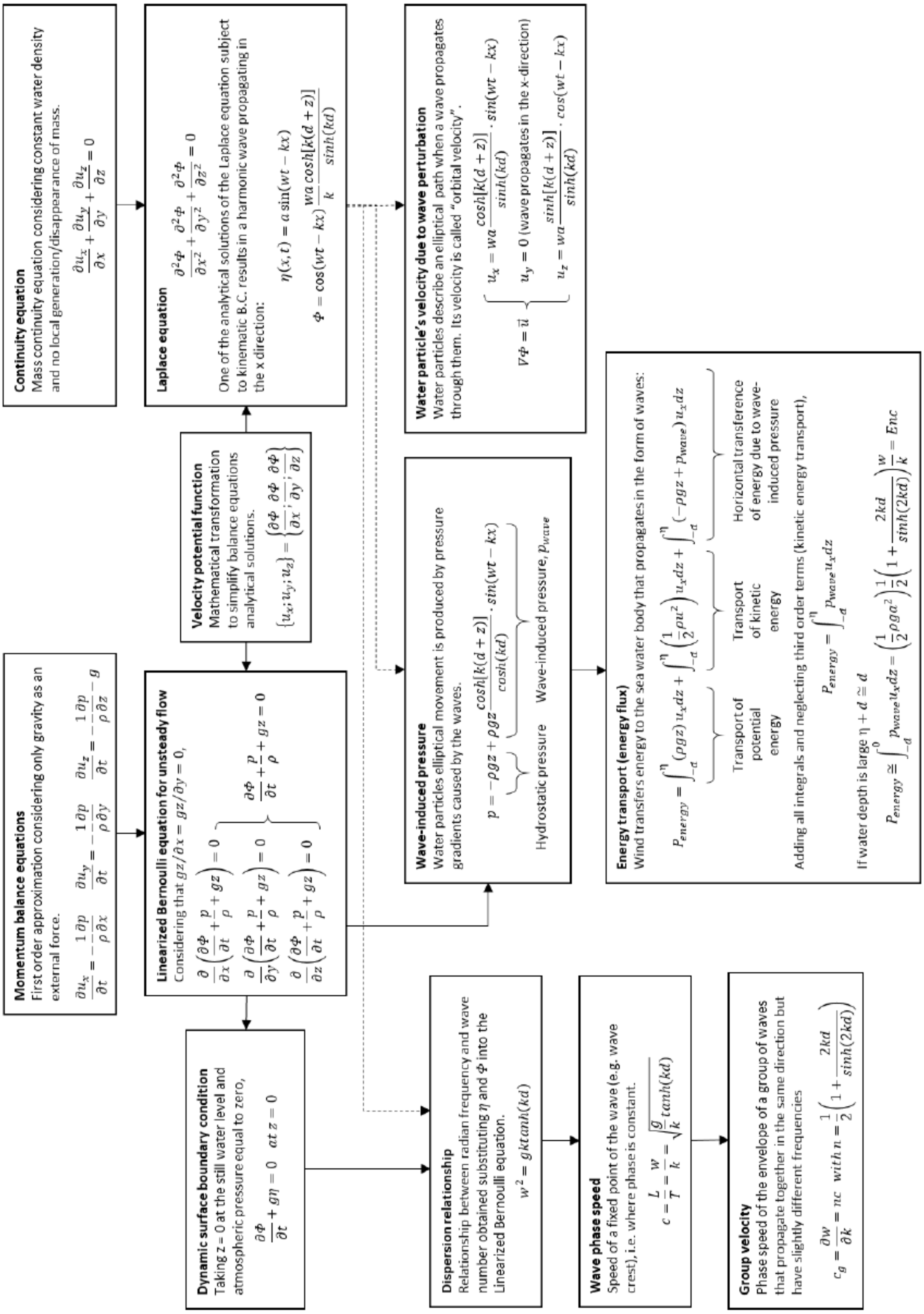

Figure 15: Flow diagram that details how the equation that describes wave energy transport is obtained (Dashed arrows have the same meaning as continuous arrows). *Source: Grases, 2017 from Booij, 1999; Holthuijsen, 2007 and The SWAN team, 2018).*

radian frequency θ.

Then, the absolute radian frequency of the wave, named w (fixed frame of reference), is:

$$w = \sigma + kU_n \tag{13}$$

Where $k = 2\pi/L$ is the wave number and U_n is the current velocity.

Distributing the wave energy density over the relative radian frequency allows to define a magnitude that does not change when a wave propagates over an ambient current. This is the wave action density, N:

$$N(\sigma, \theta; x, y, t) = \frac{E(f, \theta; x, y, t)}{\sigma} \tag{14}$$

The wave action balance equation has the same terms as the previous energy balance equation plus an additional term c_σ which accounts for relative radian frequency variations due to depth and current velocity changes (frequency-shifting). This is because to define the wave action balance the frame of reference is neither fixed nor moving at the current velocity, instead is moving at the same velocity of the wave action (or the wave energy) which is the group velocity.

$$\frac{\partial N}{\partial t} = -\frac{\partial c_g, xN}{\partial x} - \frac{\partial c_g, yN}{\partial y} - \frac{\partial c_\theta N}{\partial \vartheta} - \frac{\partial c_\sigma N}{\partial \sigma} + S \tag{15}$$

Where, again, the first term is the change of action density in the cell, the second and third term are the net import of action density due to unidirectional propagation, the third term is the net import of action density due to refraction and diffraction induced wave turning, the fifth term is the net import of action density due to frequency-shifting and the sixth one is the local generation/dissipation of action density.

3.3.1.1 Coastal processes - how the propagation works

Bottom induced shoaling

When waves approach the coastline their radian frequency remains constant since wave period is not altered during propagation. However, as water depth decreases wave length it is also reduced according to the dispersion relationship:

$$w^2 = gk \tanh{(kd)} \tag{16}$$

$$\text{if } w = ct. \text{ and } d \downarrow, \text{ then } k \uparrow$$
$$\text{Since } k = \tfrac{2\pi}{L},\ L \downarrow$$

The reduction of the wave length is translated to an initial increase of the group velocity followed by a continuous reduction of its value towards a theoretical null value at the coastline[3]

[3]It is physically not feasible since it would lead to an infinitely large wave amplitude. However, in the wave model it is never reached thanks to wave breaking.

Conceptually, the fact that the wave slows down produces a concentration of the wave energy in the area in front of the coast and, consequently, an increase of the wave amplitude.

Therefore, wave shoaling is directly taken into account in the SWAN model by the group velocity term itself, which depends on the water depth.

Bottom induced shoaling

Refraction is produced when a wave front propagates obliquely towards a coastline. Wave crests that are closer to the shoreline have a smaller phase velocity than those which are further from the shoreline, since phase velocity diminishes when water depth decreases. Then, the angle between the wave front and the shoreline is progressively reduced because the part of the front that is further from the shoreline travels faster. At the end, the wave front becomes parallel to the coastline.

In the SWAN model refraction is visualized as a progressive transference of energy density (or action density) from an initial direction (the direction of propagation of the wave front in open sea) to a final direction (that of a wave front parallel to the coast). In other words, there is a shift in wave energy transport direction.

Refraction is accounted for using the so called refraction-induced directional turning rate per unit time:

$$c_{\theta,ref} = [\frac{d\theta}{dt}]_{ref} = -\frac{c_g}{c}\frac{\partial c}{\partial m} \tag{17}$$

Where m corresponds to a local coordinate oriented along the wave crest. Thus, $\partial c/\partial m$ is the variation of the phase velocity along the wave crest.

Diffraction

Diffraction occurs when a wave front encounters an obstacle, such an emerging group of rocks or a breakwater. Since waves cannot overcome the obstacle there is no direct transfer of energy behind it and a "shadow zone" is created. However, when a wave front passes by its side it transfers energy to this area which causes the wave front to curve behind the obstacle forming a circular wave pattern with decreasing amplitude.

For a harmonic unidirectional wave this phenomena is modelled considering a parameter $\Im_a$ that accounts for a decrease of the phase speed in the shadow area.

$$C = \frac{c}{\sqrt{(1 + \Im_a}} \tag{18}$$

with

$$\Im_a = \frac{\nabla^2 a}{k^2 a}\frac{\partial^2 a/\partial x^2 + \partial^2 a/\partial y^2}{k^2 a} \tag{19}$$

Where C is the modified phase speed due to diffraction.

The effect of diffraction on the group velocity is modelled in the same way:

$$CC_g = \frac{c_g}{\sqrt{(1 + \Im_a}} \tag{20}$$

This approach to compute the diffraction poses an important problem: wave amplitude is used to compute diffraction but diffraction is needed to compute wave amplitude (since wave amplitude is one of the main outputs of the model). Besides, it has been shown (Goda, 2000) that for a realistic situation with random short-crested waves that propagate towards the obstacle from several directions (instead of considering a single harmonic unidirectional wave), wave height in the shadow area is much smaller since their individual contributions are partially counterbalanced due to wave interaction. Both problems are solved in SWAN model replacing the amplitude by the square root of the energy density, which leads to a modified diffraction parameter, $\Im_E$.

$$a \cong \sqrt{E(f)} \rightarrow \Im_E = \frac{\nabla^2 \sqrt{E(f)}}{k^2 \sqrt{E(f)}} \tag{21}$$

Finally, the diffraction is introduced in the SWAN model with an analogous parameter to that used for the refraction: the diffraction-induced directional turning rate.

$$c_{\theta,dif} = \frac{C_g}{2(1+\Im_E} \frac{\partial \Im_E}{\partial m} \tag{22}$$

Nevertheless, to precisely compute diffraction alternative models such as the Boussinesq type models or those based on the mild-slope equations shall be used. However, their computational cost is much higher and are not operational except for pretty small study domains.

Reflection and transmission

An obstacle may reflect, transmit and absorb wave energy in different proportions depending on its nature. For example, a beach with a gentle slope absorbs almost all wave energy while an emerged vertical breakwater reflects most of it. Besides, detached structures from the coast can transmit part of the incident wave energy depending on its height and porosity.

The energy balance of a wave train that reaches an obstacle is described below:

incident energy (reflected energy + transmitted energy) = absorbed energy

In case of perfect energy reflection of a single harmonic unidirectional wave (incident energy = reflected energy), a standing wave is generated.

$$\eta(x,t) = a_i \sin(wt - kx) + a_r \sin(wt - kx) = 2a_i \cos(kx) \sin(wt) \tag{23}$$

Where a_i and a_r are the amplitudes of the incident and reflected waves, respectively ($a_i = a_r$).

However, as it has been stated, perfect energy reflection is not observed in nature ($a_i > a_r$). For a single harmonic unidirectional wave, a partially standing wave would be generated. It is described as the sum of a complete standing wave plus a simple harmonic wave with a smaller amplitude than the incident wave. This way, the maximum amplitude of the standing wave, at its nodes, is reduced, whereas there are no longer perfect antinodes.

$$\eta(x,t) = a_i \sin(wt - kx) + a_r \sin(wt - kx) = 2a_i \cos(kx) \sin(wt) \tag{24}$$

The reflection coefficient is then defined as the ratio between the reflected wave and the incident wave:

$$K_{reflection} = \frac{a_r}{a_i} \tag{25}$$

Because of the complexity of this phenomenon, this coefficient it is generally obtained though observations using the Iribarren parameter ε, which relates the beach slope with the wave steepness.

Dissipation
Wave energy dissipation is produced by three phenomena apart from energy absorption in obstacles: white-capping, bottom friction and wave breaking. White-capping is a highly non-linear phenomenon in which waves experience a partial breaking (i.e. wave height is reduced) which is not triggered by the proximity to the sea bottom. Although it seems that wave steepness has a maximum threshold ($H_{max}/L \approx 0.14$ in deep water), there is not a clear correlation between wave steepness and white-capping. In SWAN, this phenomenon is modelled using a white-capping source term based on the theory of (Hasselmann, 1974):

$$S_{wc}(\sigma, \theta) = -\mu k E(\sigma, \theta) \tag{26}$$

Where E(σ, θ) is the wave energy density, k is the wave number and μ is a coefficient that depends on a parametric equation in which it is accounted the wave steepness among other factors.

Bottom friction is the main mechanism for wave energy dissipation and it is also implemented in SWAN using a source term:

$$S_{bfr}(\sigma, \theta) = -\frac{C_{bfr}}{g}[\frac{\sigma}{sinh(kd)}]^2 E(\sigma, \theta) U_{rms,bottom} \tag{27}$$

Where C_{bfr} is a bottom friction coefficient and $U_{rms,bottom}$ is the root mean square orbital velocity at the bottom.

Finally, wave breaking is modelled imposing a maximum wave height through the following expression:

$$H_{max} = \gamma(d + \overline{\eta}) \tag{28}$$

Where d is the water depth below the mean sea level, $\overline{\eta}$ is the sea surface elevation (which includes wave set-up) and γ is a breaking index which is obtained from laboratory and field experiments (it is said to depend on wave steepness and beach slope). γ has a default value of 0.73 in SWAN.

Triad wave-wave interactions
Triad wave-wave interactions result from a very complex non-linear mechanism of energy transference among waves due to a resonance phenomenon.

Triad interactions require a combination of three freely propagating waves so that the sum of frequencies and wave numbers vectors of two first wave components are equal to the frequency and wave number vector of the third component, conditions that only develop in very shallow water. Then, the quantity of energy transferred depends on the phase differences among the participating waves.

Another kind of nonlinear wave-wave interactions are the quadruplets, which are produced both in deep and finite-depth water, but not in very shallow water."

3.3.2 Vegetation model

Regarding the vegetation, the first step to perform is to define the zone where it is going to be planted. This space can be seen in the Figure 12 and more precisely in Figure 16. This area, of approximately 1 km^2, has been defined with the Zostera noltii limitations and our objective coast of protection, Mangalia beach. The vegetation is a limitation due to its minimum and maximum deep where it can live, in our case the Zostera noltii species range is from 1 to 10 m deep (Short et al., 2010). But in a study from Romania, therefore closer to our conditions, the maximum is considered 6 m deep (Nita et al., 2014). Also, being a beach with a lot of tourism and a lot of use in the summer season, it is decided to put the minimum at 2 m deep. This prevents it to disturb the swimmers and tourists.

Figure 16: Position of the vegetation mask. *Source: Self-made using Google Earth.*

But there is more information apart from the placement that SWAN needs towards modeling the wave attenuation due to vegetation correctly. This information is plant height, 20 cm; section area of the plant, 2 cm^2; density of stems in the placement area, 100 stems/m^2; and drag coefficient, 0.095.

The plant height and section area values are extracted from Short et al. (2010) and Nita et al. (2014). Regarding the density, there is less precise information about it, in those two commented papers there is a vague description of the plant field and do not go into density details. Nevertheless other similar studies (Koftis et al., 2013; Kobayashi et al., 1993; Fonseca and Cahalan, 1992 and Castell, 2018) have determined a commonly accepted range of density between 50 and 100 stems/m^2. In our case the 100 stems/m^2 is chosen as the trend seems to go in this direction looking at the references and this place is catalogued as very suitable for planting or transplanting Zostera noltii (Nita et al., 2014).

Finally the drag coefficient has been calculated following Myrhaug and Holmedal (2011). As it depends almost completely on the vegetation field parameters and not on the hydrodynamic conditions is the same coefficient for every case.

4 Study Area

4.1 Site description

4.1.1 The Romanian coast

As one may know, Romanian coast is located in the west part of the Black Sea, between the Danube river and Vama Veche, see Figure 17. This coastline is only roughly 244 km long, and although it may seem short compared to, for example, the coast of Spain -which is 5,978 km long approximately- the Romanian coast have a important role in the ecosystem of the zone and for the economic development of the country (Charlier and De Julio, 1985 and Gastescu, 1993). It is so important mainly for three reasons: the Danube Delta Biosphere Reserve, the importance of the coast for the tourism and its repercussion in the Romanian GDP (Surugiu and Razvan, 2013), and the Port of Constanța which is the entrance of most imported goods.

Figure 17: Romanian coast location. *Source: Self-made from Google Earth.*

As it has been explained, the seashore extends from the Chilia branch on the Danubian Delta -north border- to Vama Veche -south border-. It is divided in two main units using geographic and geomorphic criteria: the northern unit, the Danube Delta one, and the southern unit (RCMGG, 1994). Starting from the north, in the Romanian coast one finds first the northern unit which comprehends the Romanian part of the Danubian Delta Biosphere Reserve which is divided between Romania and Ukraine. This Biosphere Reserve extends from the north Romanian border in the Chilia branch until the Midia Cape. Following this first unit one finds the southern unit, it extends from the Midia Cape until Vama Veche (Coman, 2006). It is divided in two main sectors: the Mamamia-Port Constanța sector and Constanța-Vama Veche sector.

The northern unit -Danubian delta- coast is still a very virgin zone without a clear defined sea shore as the wetlands, lakes and reed beds of the delta merge with the Black Sea. This place is considered the largest wetland of Europe and also includes fixed and mobile sand dune areas (Panin, 1998; Dan, 2013 and Pons, 1992). There are three significant distributaries which there lobes form the delta, Chilia, Sulina and Sfantu Gheorghe (Bondar and Panin, 2001), see Figure 18. Its net longshore sediment transport along the Danubian coast is high on average and it is almost unidirecctional to the south (Giosan et al., 1999).

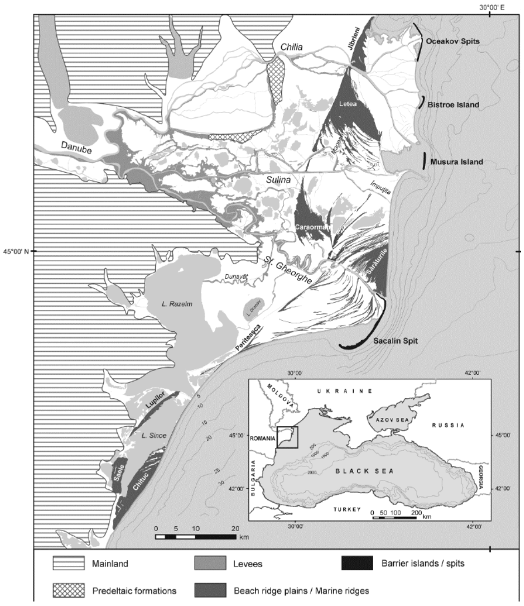

Figure 18: Danubian delta geography and its distributaries. *Source: Vespremeanu-Stroe and Preoteasa, 2015.*

Regarding the southern unit, just after Midia Cape, one finds the Mamamia-Constanța sector, it is considered transitional with high cliffs separated by large accumulatives beaches which in some cases are backed by litoral lakes. The most important beach in this sector, of 8 km long, is the Mamaia beach: a narrow sand bar 250-300 m wide between the Black Sea and Siutghiol Lake. It is strongly influenced by the Midia harbour jetties (Coman et al., 1999). As the harbour protection dikes trap the longshore sediment transport causing sediment starvation of the entire Romanian Southern Coastal Zone where most public beaches and tourist activities were developed. This zone is more stable in comparison with the northern, deltaic coast and is formed for an almost continuous loess cliff up to 12-20 m high. Before the construction of some shore protection facilities in this sector the cliff line was retreating with an average rate of 50 cm/year (Selariu, 1971 and Serbãnescu, 1969, in Kosyan Panin, 1996) but now is more stabilized.

The second sector (Constanța-Vama Veche) shores, south of the Constanța Port, receive no sandy sediments from the Danube. As there is no other source of supplying siliciclastic sand material, the shore deposits of this area are of an organic origin, originating from the mechanical grinding of the littoral shells. This sector was having an average of -0.6 m/year rate of the shoreline position change, negative meaning erosion, between the period 1924 to 2002 (JICA, 2005). If this rate had continued in the past thousand years then it means than the coastline have retreated 600 m. Anyway, after the implementation of some protection facilities this rate has decreased, especially in Eforie where there were made more protection related works and projects (JICA, 2007).

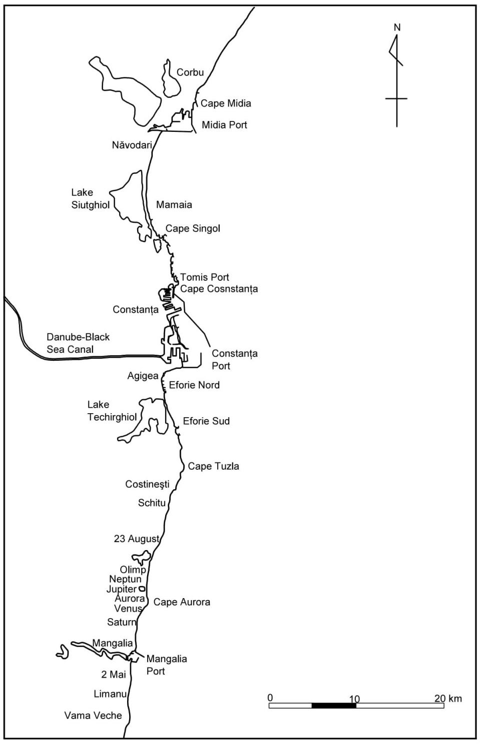

Figure 19: Map of the Southern Unit of the Romanian coast. *Source: JICA, 2005.*

4.1.2 Mangalia-Saturn seashore

The Mangalia-Saturn seashore is situated in the second sector of the southern unit of the coast of the Romanian coast. Located between the Mangalia port and the Aurora Cape, in the 43^{o}49'48"N 28^{o}35'16"E coordinates, see Figure 20.

Figure 20: Map of the Mangalia-Saturn seashore. *Source: Self-made from Google Earth.*

As one can see from the satellite images, in this small piece of coast of about 5 km long there is fifteen erosion protective structures: fourteen jetties and one detached breakwater. This amount of investment made in this small zone indicates how important it is for the economic development of the region to have a large beach. It is clear that tourism has an important role in the economy of the region (Surugiu and Razvan, 2013). Before 1985 it had only one big beach at the north side of the Mangalia Port and lake Mangalia was separated from the sea by a short barrier beach.

In this zone bivalve shell fragments and rock fragments -clasts- of limestones are the primary and secondary source of beach sand and at it has been stated there is no sand from Danubian delta (JICA, 2005).

Water level and Astronomical tide has been measured on Constanța Port since 1933 by different national organisms. Also there is data from the NIMRD -National Institute for Marine Research and Development- from the hourly water level in Mangalia Port since 1991. The mean sea level sits around 0.233 m and as it is indicated at JICA (2005) the Astronomical tide amplitudes are small compared to the water fluctuations. Another interesting tendency one can see from the data is the rise of the mean water level since 1933. It has increased more than 16 cm over 85 years and this increment must have contributed to the coastline retreat in the area.

Regarding the temperature and precipitation, the statistical data extracted from the 'Romanian Statistic Yearbook' shows that exist influence by the presence of the Black Sea, having an annual air temperature variation smaller than inland the country. The mean temperature on this zone during the year is 11.3 degrees Celsius. Precipitation averages out at 380mm and is also relatively lower than inland the country, nevertheless heavy rains in the coast caused cliff erosion and flooding problems in recent years, increasing the deterioration of the coast.

The National Agency of Meteorology calculate a mean wind speed of 5.5 m/s, predominating those from NNW to NE in this area. Also more stronger winds superior to 10 m/s appear frequently from the north direction. One can see the wind rose based on the ECMWF -European Center for Medium Range Weather Forecasting- hindcast data in Figure 21.

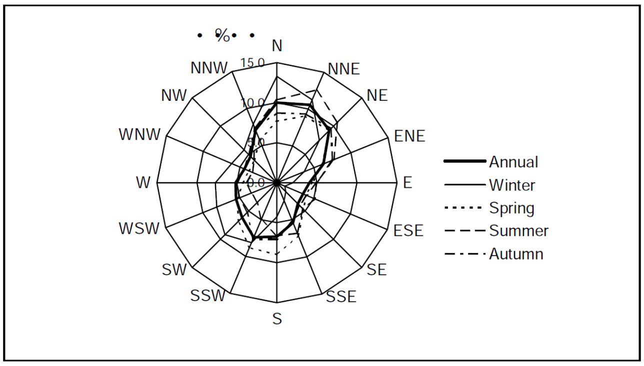

Figure 21: Directional distribution of wind frequency (in percentage). *Source: ECMWF -European Centre for Medium-Range Weather Forecasts-.*

4.2 Wave Climate

As it has been explained in the methods section, for this numerical analysis is used data from no extremal climate as when there is a storm case the seagrass does not mitigate the wave energy as it does with no extremal cases. Nevertheless is necessary to understand the wave climate in general in order to better comprehend the area of study.

The Black Sea is considered a dynamic environment where it exist seasonal and inter-annual wave energy budget changes (Onea and Rusu, 2017). In Halcrow Romania (2011) study, that used 18.5 years of hindcast dataset obtained from Fugro-Oceanor, it is estimated a larger offshore wave height for long term average approach in the north (0.85 m) than the south of the coast (0.95 m). Estimating also the maximum wave height higher in the south compared to the north.

As it is supposed, summer (April - October) is the calmest period of the year. In opposition to this, the roughest period is winter time (November - March). The highest waves from the south are related to this winter period (Halcrow Romania, 2011).

Month	Mean waves		10% exceedance wave		1% exceedance wave	
	ECMWF	NIMRD	ECMWF	NIMRD	ECMWF	NIMRD
January	1.11 m (5.1 s)	1.30 m (5.1 s)	2.0 m (6.8 s)	2.5 m (6.8 s)	4.4 m (9.1 s)	4.9 m (8.1 s)
February	1.06 m (5.1 s)	1.02 m (5.0 s)	2.0 m (6.7 s)	1.7 m (6.6 s)	3.6 m (8.4 s)	3.8 m (7.8 s)
March	1.05 m (5.2 s)	1.05 m (5.1 s)	1.8 m (6.8 s)	2.2 m (6.8 s)	3.7 m (8.2 s)	3.4 m (8.1 s)
April	0.88 m (5.1 s)	0.74 m (4.5 s)	1.6 m (6.6 s)	1.4 m (6.4 s)	2.9 m (8.0 s)	2.5 m (7.6 s)
May	0.71 m (4.8 s)	0.77 m (4.4 s)	1.4 m (6.4 s)	1.5 m (5.8 s)	2.6 m (7.8 s)	2.5 m (7.2 s)
June	0.65 m (4.5 s)	0.65 m (4.2 s)	1.3 m (5.8 s)	1.3 m (5.8 s)	2.2 m (7.3 s)	2.3 m (7.0 s)
July	0.68 m (4.5 s)	0.62 m (4.1 s)	1.4 m (6.1 s)	1.0 m (5.5 s)	2.3 m (7.5 s)	1.9 m (6.9 s)
August	0.73 m (4.8 s)	0.73 m (4.3 s)	1.4 m (6.2 s)	1.4 m (5.6 s)	2.3 m (7.8 s)	2.2 m (6.8 s)
September	0.89 m (4.9 s)	0.90 m (4.6 s)	1.7 m (6.6 s)	1.8 m (6.0 s)	3.1 m (8.0 s)	3.2 m (7.4 s)
October	1.03 m (5.2 s)	1.03 m (4.7 s)	2.0 m (6.9 s)	1.9 m (6.3 s)	3.4 m (8.6 s)	4.0 m (7.7 s)
November	1.18 m (5.3 s)	1.14 m (5.0 s)	2.4 m (7.2 s)	2.3 m (6.8 s)	4.4 m (9.4 s)	4.2 m (8.2 s)
December	1.31 m (5.5 s)	0.97 m (4.9 s)	2.7 m (7.4 s)	1.9 m (6.4 s)	4.9 m (9.5 s)	3.6 m (7.7 s)
Winter (Nov. – Mar.)	1.16 m (5.2 s)	1.10 m (5.0 s)	2.3 m (6.9 s)	2.2 m (6.7 s)	4.4 m (9.0 s)	4.1 m (8.0 s)
Summer (Apr. – Oct.)	0.79 m (4.8 s)	0.78 m (3.8 s)	1.5 m (6.5 s)	1.5 m (5.5 s)	2.8 m (7.9 s)	2.8 m (7.0 s)
Whole year	0.95 m (5.1 s)	0.91 m (4.7 s)	1.8 m (6.6 s)	1.8 m (6.3 s)	3.6 m (8.4 s)	3.5 m (7.8 s)

Table 12: Monthly, seasonal and yearly characteristic wave heights and periods. *Source: JICA, 2007.*

It exists a consensus in the scientific literature which suggest that there is a trend of increasing wave energy levels and related to this and increase of wave height over the last few decades (Halcrow UK, 2011-2012; Halcrow Romania, 2011; JICA, 2008 and Onea and Rusu, 2017). This statement is really supported by Onea and Rusu (2017) study, as it uses reanalysis data from the ECMWF and satellite measurements that consider values over more than 38 years.

It is important to indicate again the small contribution of tidal effect in the water level, being estimated as only 0.05 m regarding the spring tidal range (JICA, 2008).

Mention also some information about wind, a basic element of the wave climate. In the center of the Romanian Coast is where the long term average wind speed is maximum, about 6 m/s, being reduced towards the northern and southern part of the coast. It is also shown a similar trend for the maximum wind speeds (Halcrow Romania, 2011).

5 Results

5.1 NE low energy

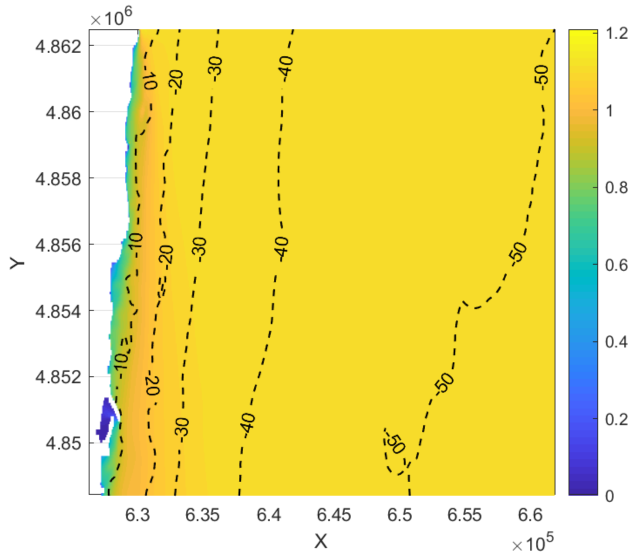

(a) Hs = 1.15m ; Tp = 5s ; Dir. = 45°

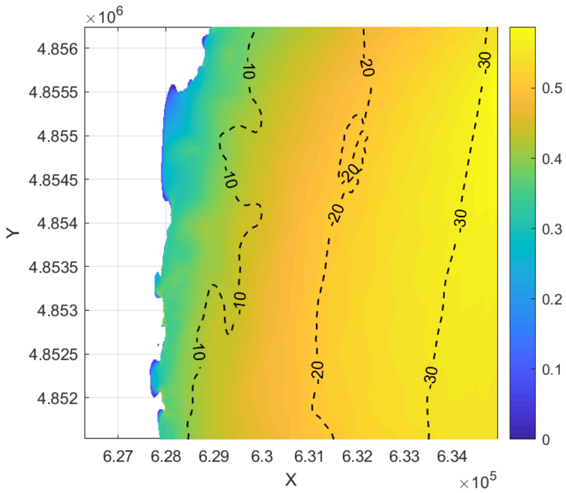

(b) Baseline scenario

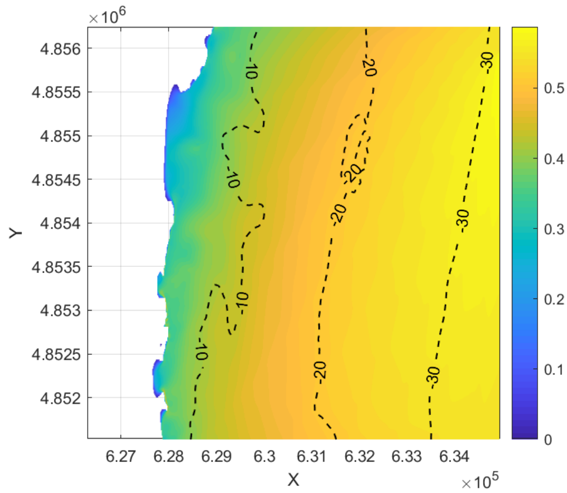

(c) Vegetation scenario

Figure 22: NE low energy. Caption of the propagation in the DOM1 (a) and its nesting with (c) and without (b) vegetation in the DOM2.

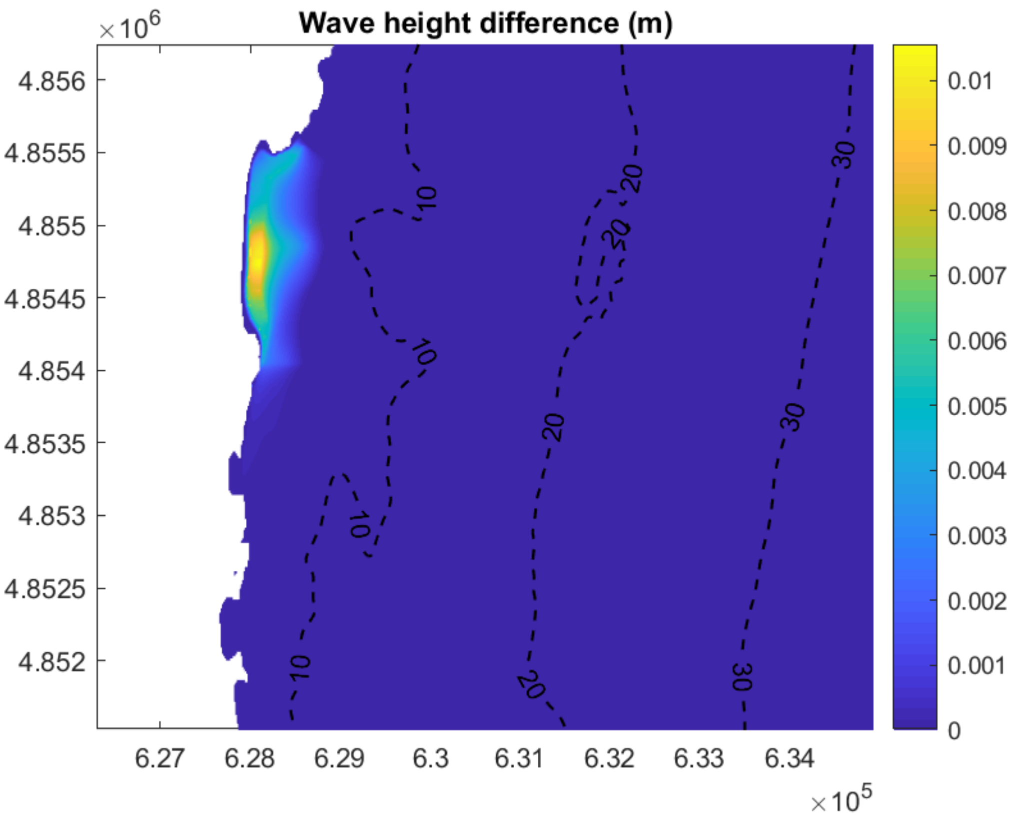

Figure 23: NE low energy. Comparison between (b) and (c).

5.2 NE moderate energy

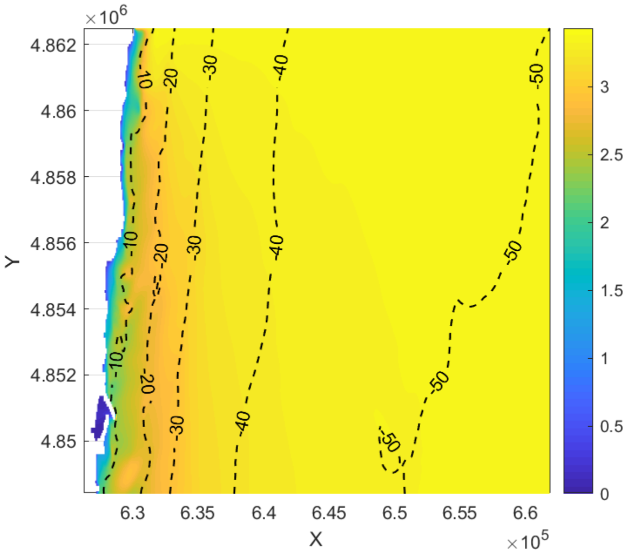

(a) Hs = 3.43m ; Tp = 9s ; Dir. = 45°

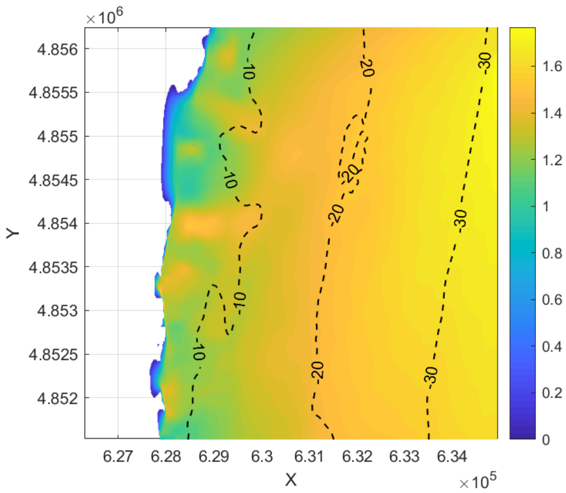

(b) Baseline scenario

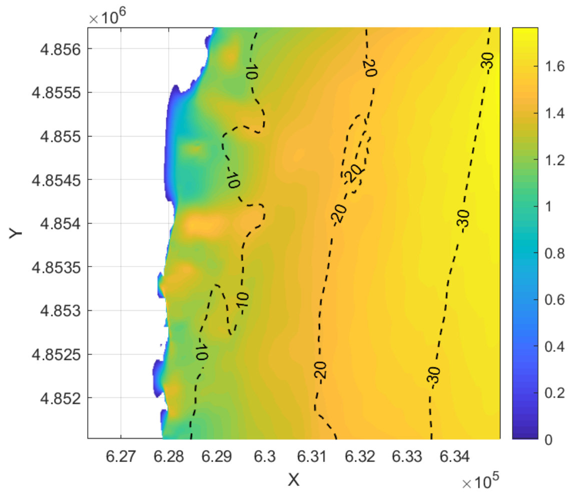

(c) Vegetation scenario

Figure 24: NE moderate energy. Caption of the propagation in the DOM1 (a) and its nesting with (c) and without (b) vegetation in the DOM2.

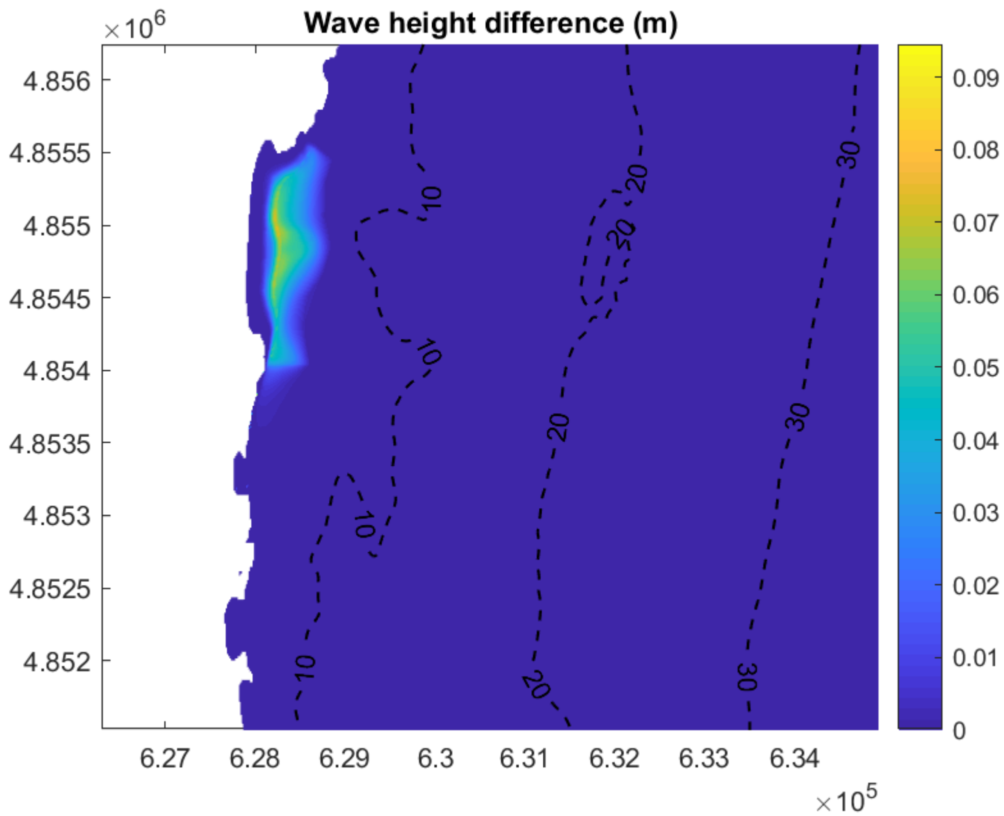

Figure 25: NE moderate energy. Comparison between (b) and (c).

5.3 E low energy

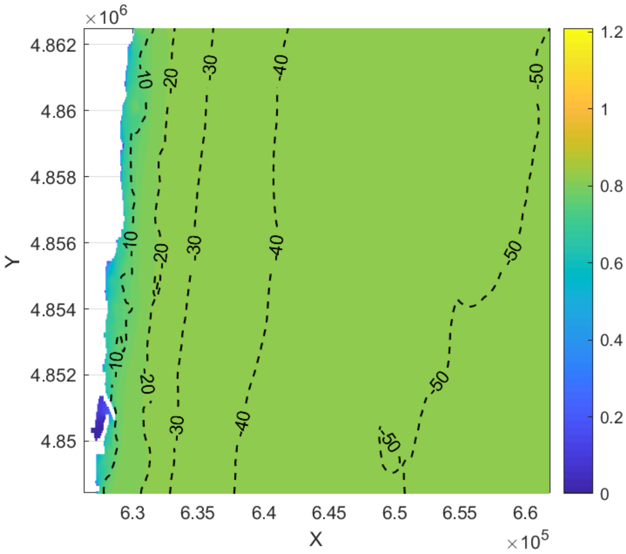

(a) Hs = 0.85m ; Tp = 5s ; Dir. = 90°

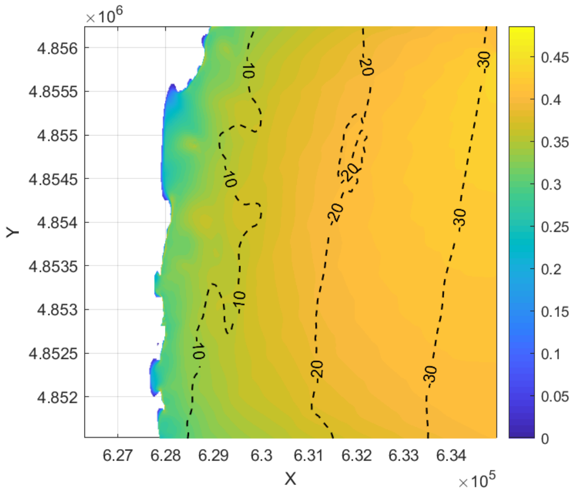

(b) Baseline scenario

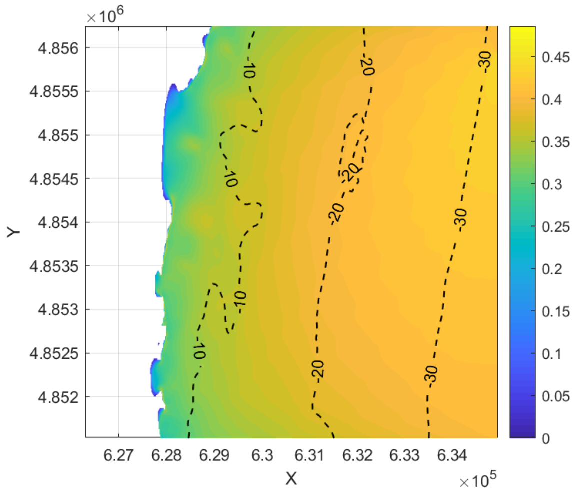

(c) Vegetation scenario

Figure 26: E low energy. Caption of the propagation in the DOM1 (a) and its nesting with (c) and without (b) vegetation in the DOM2.

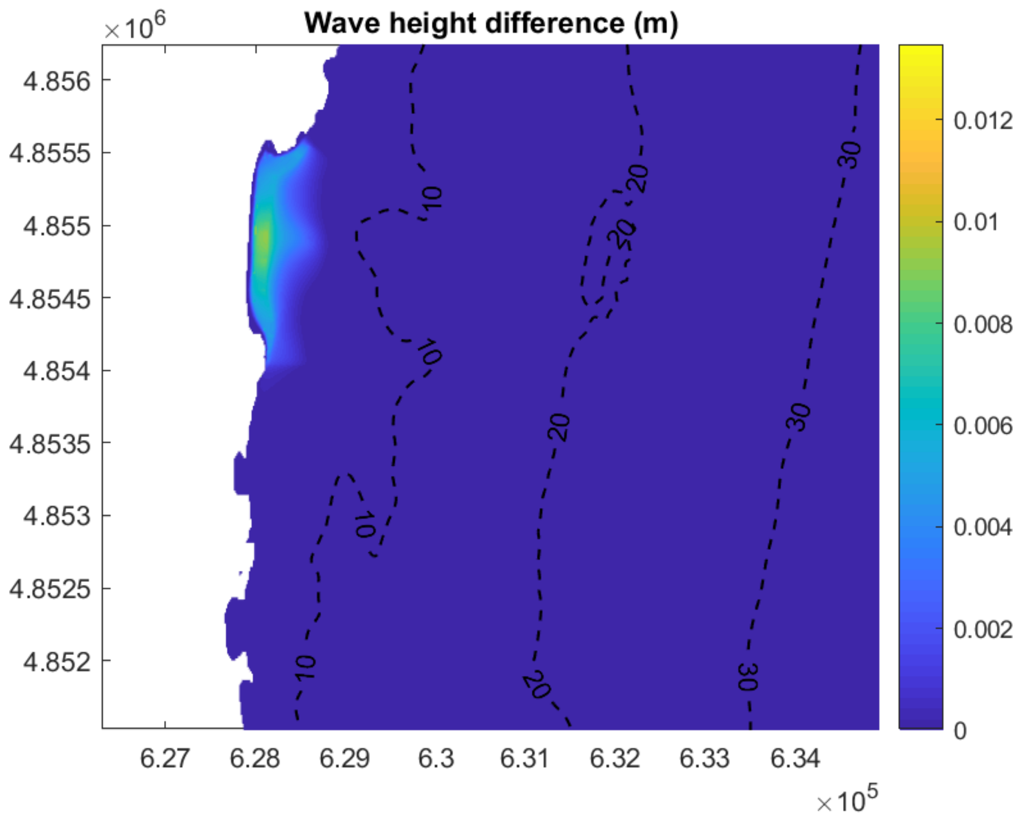

Figure 27: E low energy. Comparison between (b) and (c).

5.4 E moderate energy

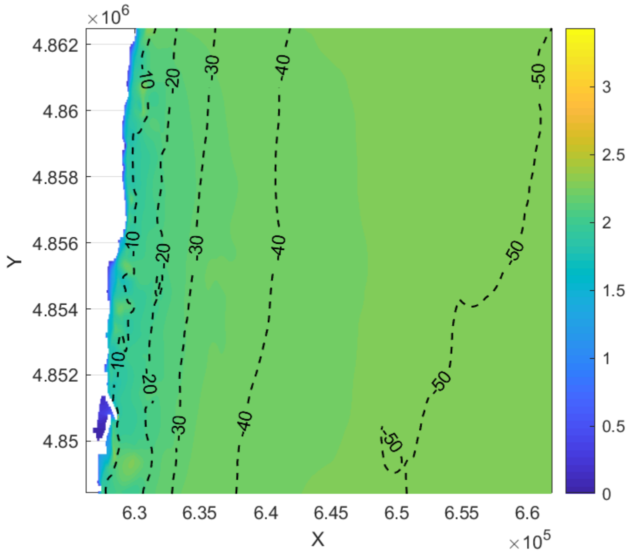

(a) Hs = 2.33m ; Tp = 9s ; Dir. = 90°

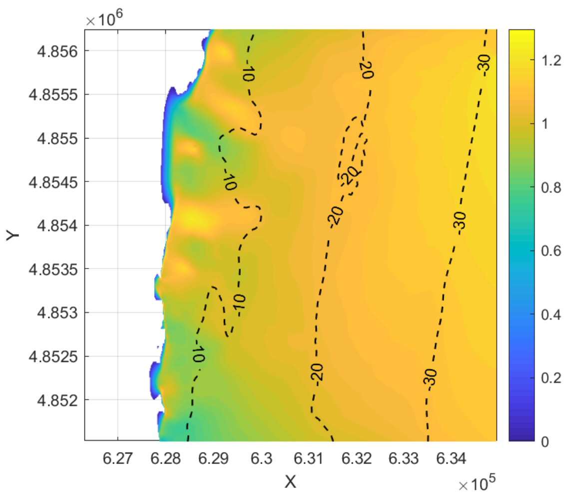

(b) Baseline scenario

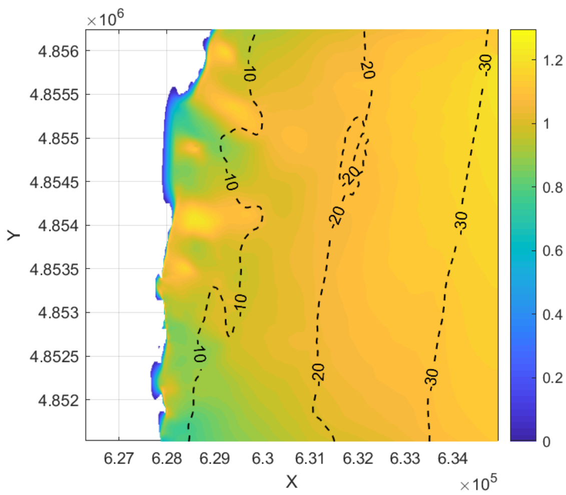

(c) Vegetation scenario

Figure 28: E moderate energy. Caption of the propagation in the DOM1 (a) and its nesting with (c) and without (b) vegetation in the DOM2.

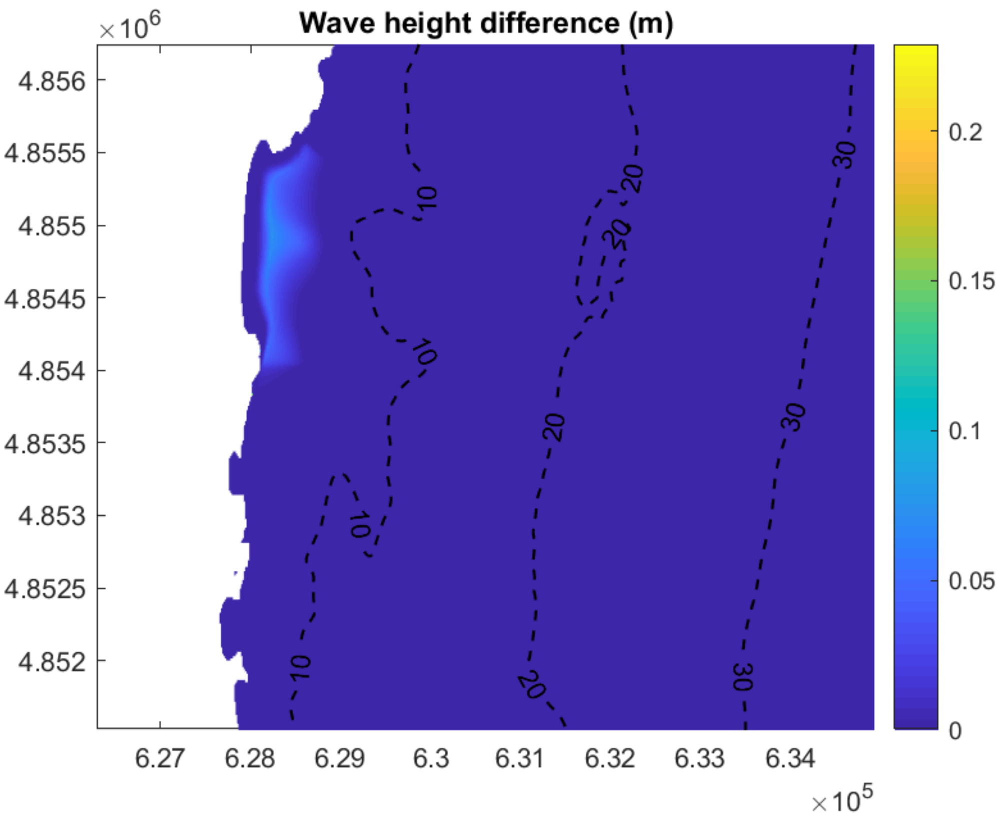

Figure 29: E moderate energy. Comparison between (b) and (c).

5.5 SSE low energy

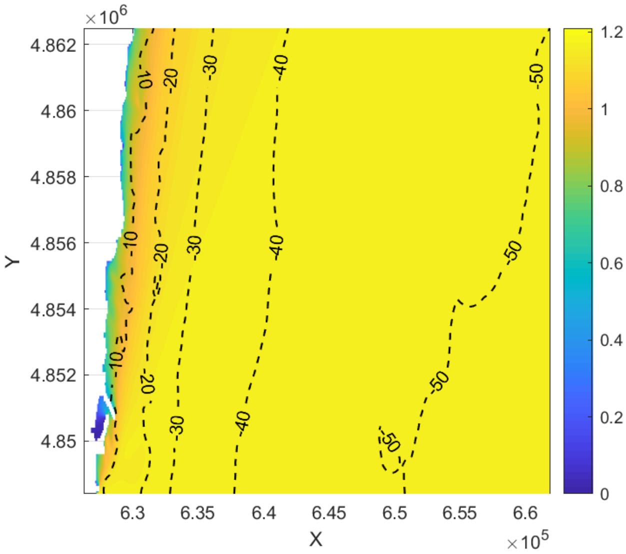

(a) Hs = 1.21m ; Tp = 5s ; Dir. = 157.5°

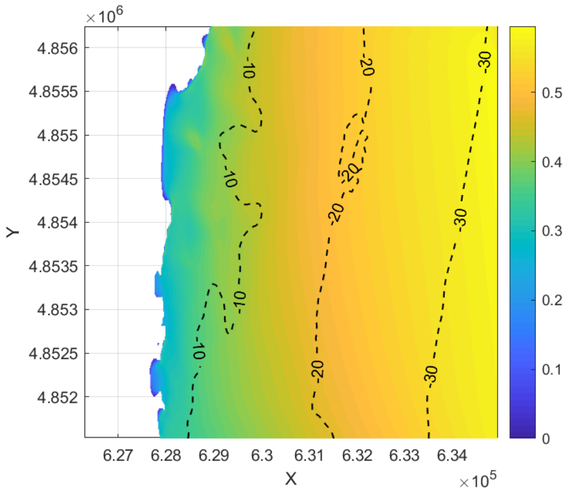

(b) Baseline scenario

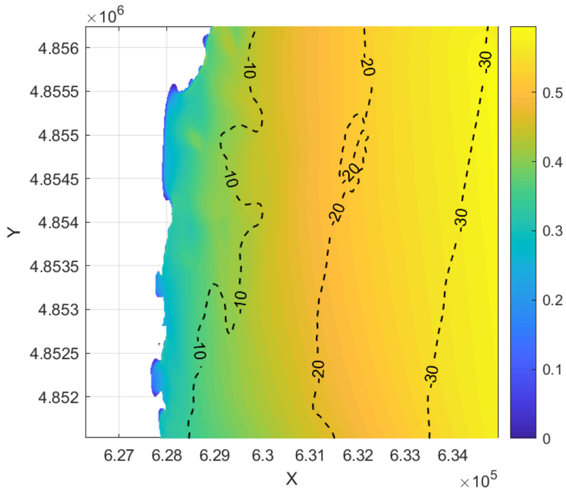

(c) Vegetation scenario

Figure 30: SSE low energy. Caption of the propagation in the DOM1 (a) and its nesting with (c) and without (b) vegetation in the DOM2.

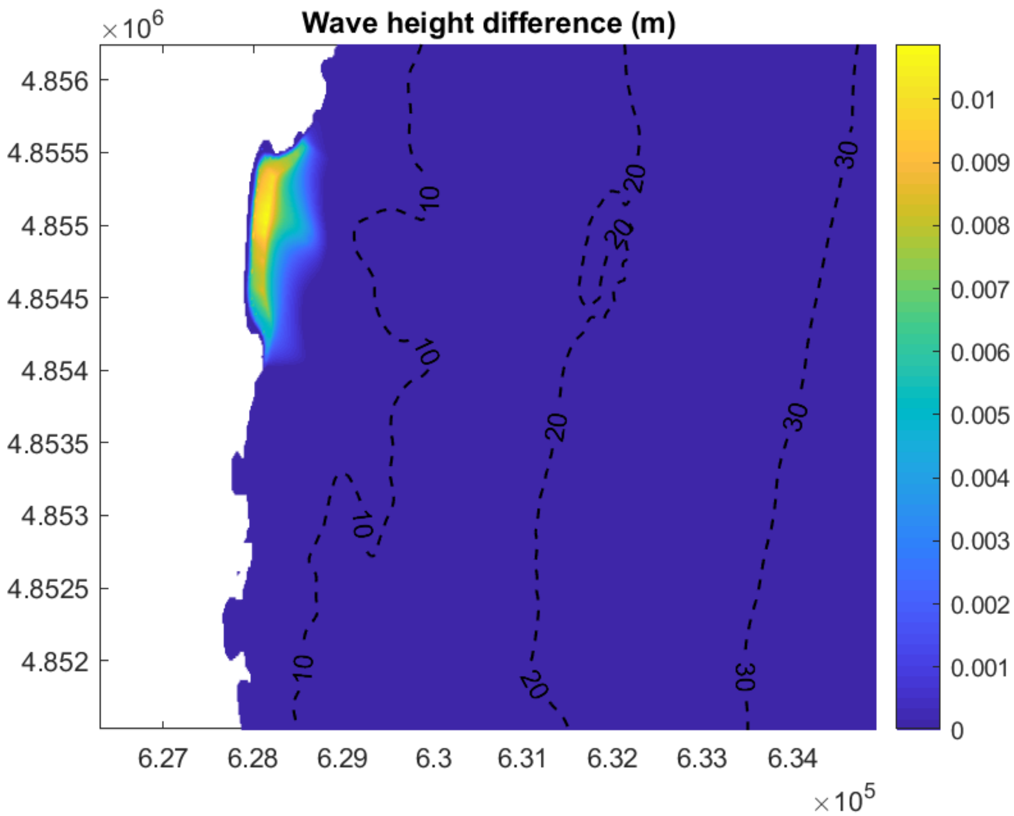

Figure 31: SSE low energy. Comparison between (b) and (c).

5.6 SSE moderate energy

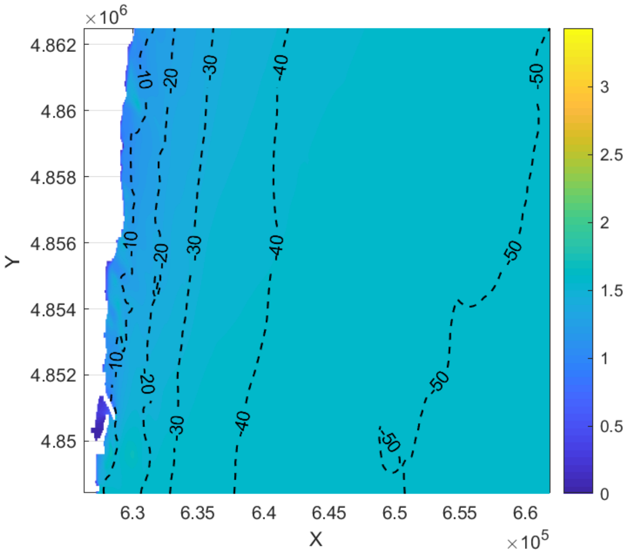

(a) Hs = 1.63m ; Tp = 9s ; Dir. = 157.5°

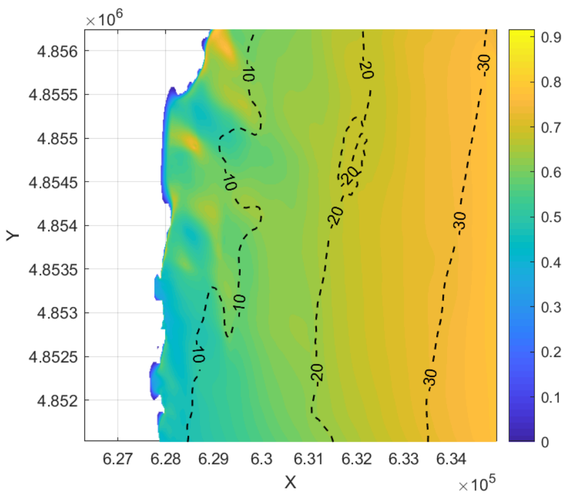

(b) Baseline scenario

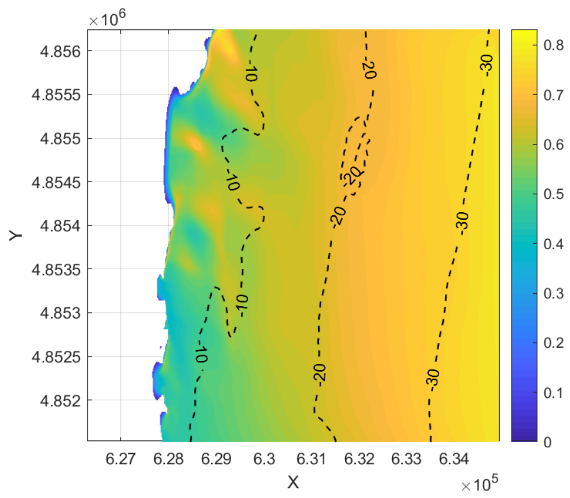

(c) Vegetation scenario

Figure 32: SSE moderate energy. Caption of the propagation in the DOM1 (a) and its nesting with (c) and without (b) vegetation in the DOM2.

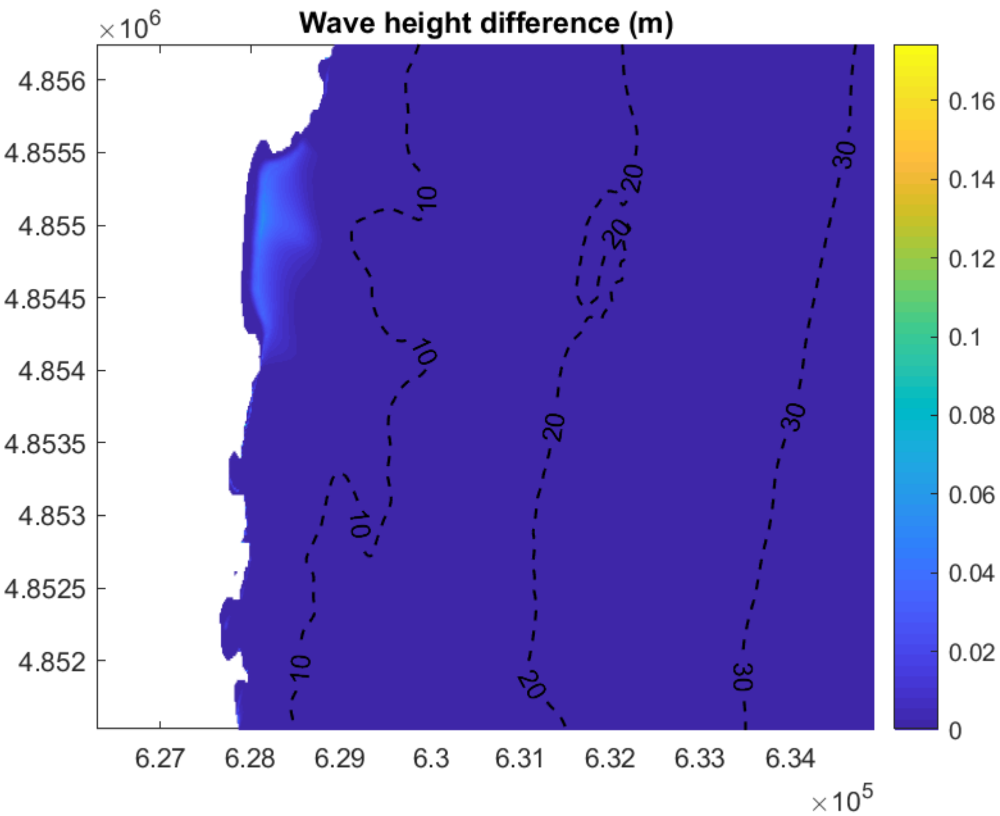

Figure 33: SSE moderate energy. Comparison between (b) and (c).

6 Discussion

The results one can see in the fifth section are obtained using SWAN and MATLAB. SWAN does the numerical propagation and outputs a series of matrices, one matrix has the wave height for each point of the model. Using this matrix and representing it in MATLAB one obtains the three first images shown in every direction and wave energy, then calculating the difference between them and plotting it one obtains the comparison figures.

For the DOM1 representations (Subfigures a) the scale is determined using as maximum as the mas wave height of the energy level they are, so all DOM1 representations have a maximum of 1.21 m for the low energy waves and a maximum of 3.43 m for the high energy waves. Then for the subfigures b and c the maximum is determined as the maximum wave height it has, so as the DOM2 has the same input for every case it remains consistent between them. Finally the scale of comparison figures is chosen using the maximum wave height difference of every figure.

The first observation that is important to point out is the difference between the low and moderate energy waves. It is consistent in all three cases an increase on the wave height difference between them, being the moderate energy the ones that reduce more wave height in the vegetation case. Nonetheless, one can see a difference in the distribution of this wave attenuation trough the seagrass between both cases. The low energy case shows a more colored -so more variable- wave attenuation where the highest difference wave height has more representation (more yellowish area). In the other hand, even if the moderate cases reduce consistently more wave height, its distribution has a predominant colour of middle scale in all three cases.

This observation has two main causes: as more energy arrives to the seagrass more energy it can damp, this is the reason moderate energy waves have a higher value of attenuation -and a higher percentage too-. The reason for it being less variable and not maximizing its results (not showing almost yellow colour) is that one of the most important variables of the vegetation for maximizing the attenuation is the difference between the end of the stems and the water level, so as the height of the plant does not change (it is 20 cm in all models) with lower waves this difference is less than the opposite.

Secondly, one can see the effect of all different waves' orientations in the subfigures (a) -DOM1 propagations- in all directions (NE, E, SSE). This means that the shoaling and attenuation from bottom friction effect can be seen as parallel lines defining lower wave height in these subfigures.

Nevertheless, in the propagations in the subfigures (b) and (c) -DOM2 propagations- these effect is less noticeable as the waves already go in a more perpendicular way to the coast. This makes the vegetation field to attenuate the waves from all directions as it has thought, only minor directional effects can be seen in the comparison figures where the direction of the waves is usually where the vegetation effect seems to be a bit wider.

Some of the numbers that seem important to point out can be observed in the next Table 13.

Table 13: Maximal and average attenuation in total and in percentage for every direction and level of energy. *Source: Self-made.*

	Max. attenuation		Ave. attenuation	
NE Low e.	0.011 m	3.3 %	0.007 m	2.4 %
NE Moderate e.	0.092 m	6.4 %	0.063 m	4.8 %
E Low e.	0.013 m	3.5 %	0.008 m	2.1 %
E Moderate e.	0.220 m	8.1 %	0.098 m	4.5 %
SSE Low e.	0.011 m	3.2 %	0.008 m	2.7 %
SSE Moderate e.	0.169 m	7.7 %	0.062 m	4.0 %

To sum up, these numbers indicate a 8 to 4% reduction of the wave height due to the seagrass field for moderate energy waves cases in all directions, and a reduction of 3.5 to 2.1% for low energy ones.

These are the main points to consider regarding our results and the main source of information that is concluded in the next section.

7 Conclusions

Green measures as the one presented in this project can serve to the mitigation of wave height and to the improvement of coast protection in the Mangalia-Saturn seashore.

Nonetheless, the results indicate a mitigation averaging around 4.4% in wave height in the moderate energy group. This is the most significant number to relate, as those are the waves which may affect more the coast, and therefore the ones that a mitigation could improve more the coast protection. It is a relevant number and it is a positive improvement but it has to be studied if this improvement could result in substantial benefits, those studies had been proposed in the Future Work section.

All directions take benefit from the vegetation field as the waves arrive to it with enough perpendicularity and there is no major coast or bathymatrial obstacle.

An improvement of this result could be achieved with different height of plants and a larger field, but the Zostera noltii proposed for this project is limited to the conditions used. Another taller seagrass which could live in more deep conditions also could mean an improvement to the results, but there is no such seagrass native from this coast, and using other species could damage the ecological resources that this green solutions are trying to protect.

Overall, although the results are positive, grey solutions are still ahead in its performance in a more controlled and stable results, as it is needed more research in this wave attenuation by seagrass field. Being this green measures a feasible solution in areas where the quantity of wave height to reduce is in the order of moderate to low.

8 Future work

1. As a first evaluation this thesis can give a good perspective of what to expect of this solution application. As a student with limited time and resources, it was not possible to perform more accurate and complex numerical modelling and data analysis. With more resources the number of nodes and the detail of the models meshes could be improved, even adding more nesting steps and more directions. Also to compute the wave model it is used a 30 years span of data, enough to calculate an accurate approximation, but having forecast and hindcast from more than a hundred years, there is room for improvement. Finally, it should be performed a calibration and a validation of the numerical model with physical laboratory models and field data.

   Implementing these upgrades could improve the detail of the work, leading it to a more extended and accurate approximation of the reality.

2. This project is centered in the reduction of the wave height due to seagrass. This wave energy reduction would lead to the improvement of the coast protection, but this is only half of the story, it should be evaluated the reduction of the impact to the coast: the sediment transport reduction, the reduction or turn back of beach demise, an other impacts on the studied area and its surroundings.

3. In order to create the vegetation mask it has been followed the instructions of previous experience and desired protection. Nevertheless, in a future work the exact shape of the vegetation mask should be analyzed taking into account the mitigation required, the space of occupation, the exact coast length it is desired to protect and should be a compromise with plants' value and its transplantation.

4. Also related to the vegetation, more research of different seagrass native to the coast and with better characteristics (taller, denser and that could survive in more depth) than Zostera noltii should be performed, as it is one unsolvable limitation for the improvement of the results found out in the project.

5. As it has been explained, there are scientific publications that endorse the transplantation of seagrass (Nita, 2014). Nonetheless a study on the transplantation or plantation of a big field of seagrass -as in our case- should be performed in order to understand and project the growing process and its resulting growing protection of the coast. Also it would introduce more data or information that would improve the estimation of the costs of the project.

6. This seagrass solution is considered a green measure to protect the coast, but there also exist grey measures. It is known that from an ecological perspective a green measure is always going to win versus a grey measure, but there are more perspectives. A cost-benefit analysis with the estimation of construction and long term costs, performances of both type of solutions, ecological value and collateral effects (like visual impact or tourism attraction) should be performed. This type of green measure is another solution for a problem that gives more flexibility and is focused in an environmental perspective, but this does not mean that it is going to be always the way to go.

7. There are a large variety of grey measures to improve the coast protection. To perform a good cost-benefit analysis as described in the fourth point, one should analyze which is the best grey measure for this case and evaluate it in a similar way to what has been made in this thesis. And should include studying the impact on coast protection and collateral problems to the coast down stream. Moreover, it should be analyzed a combination of both types of solutions for example, planting vegetation and refilling the beach once in a while.

8. This project has studied non-extremal cases regarding wave climate. It should be performed a study regarding these extremal cases and how the vegetation can mitigate them as the same time that stems loss or bending is taken into consideration.

9. A last consideration should be the authorities and universities implication and fomentation of this kind of measures. These measures are just one response to the actual main humanity problem, the ecological preservation of The Earth. Competent authorities are the ones that can turn this investigations to reality, integrating a new green measure to the existing alternatives for the reduction of coastal impacts.

References

Abele Jr, R. W., 1977. Analysis of Short-Term Variations in Beach Morphology (and Concurrent Dynamic Processes) for Summer and Winter Periods, 1971-72, Plum Island, Massachusetts.

Airy, G.B., 1841. Tides and waves. In Rose, H.J., et al., 1817–1845. Encyclopædia Metropolitana, Mixed Sciences, 3.

Blackmar, P.J., Cox, D.T., and Wei-Chang, W., 2013. Laboratory observations and numerical simulations of wave height attenuation in heterogeneous vegetation. Journal of Waterway, Port, Coastal, and Ocean Engineering, 140(1), pp. 56-65.

Bondar, C. & Panin, N., 2001. The Dnube Delta hydrologic data base and modelling. Geo-Eco-Marina, 5-6, Bucharest - Constanta, Romania, pp. 5-52.

Booij, N., Ris, R.C. & Holthuljsen, L.H., 1999. A third-generation wave model for coastal regions, Part I, Model description and validation. Journal of Geophysial Research, 104 (c4): 7649-7666.

Borsje, B.W., et al., 2011. How ecological engineering can serve in coastal protection. Ecological Engineering, 37(2), pp. 113-122.

Bouma, T. J. et al., 2014. Identifying knowledge gaps hampering application of intertidal habitats in coastal protection: Opportunities & steps to take. Coast. Eng. 87, pp. 147–157.

Castell, X., 2018. Estudio del uso de praderas submarinas como medida de protección costera. Master thesis, Universitat Politècnica de Catalunya.

Charlier, R.H. and De Julio, E.W., 1985. Romania, In: Bird, E. and Schwartz, M. (eds.), *The world's coastline.* New York: Van Nostrand Reinhold C., pp. 459-465.

Chiaia G., Damiani L. and Petrillo A., 1992. Evolution of a beach with and without a submerged breakwater: Experimental investigation - 23nd ICCE.

Christianen, M.J.A. et al., 2013. Low-canopy seagrass beds still provide important coastal protection services. Project Theseus OD3.10: Integrated report on contrasting ecological outcomes of alternative management strategies.

Coman, C., Morgan, R. & Williams, A.T., 1999. The need for beach management. A case study of Mamaia beach, Romania. Proceedings of the Joint Conference MEDCOAST'99 & EMECS'99 Land-Ocean Interaction: Managing Coastal Ecosystems.

Dalrymple, R., Kirby, J. and Hwang, P., 1984. Wave Diffraction Due to Areas of Energy Dissipation. Journal of Waterway, Port, Coastal, and Ocean Engineering, 110(1), pp. 67-79.

Dan, S., 2013. Coastal Dynamics of the Danube Delta. Ph.D. thesis, Delft University of Technology.

Dinu, I. et al., 2017. Using Numerical Modelling to Analyze Beach Profiles Response to Extreme Storms along the Danube Delta coast, Romania. Geo-Eco-Marina, 23, pp. 45-70.

Fonseca, M.S. et al., 1982. Influence of the seagrass, Zostera marina L., on current flow. Estuarine Coastal Shelf Science, 15(4), pp. 351-364.

Fonseca, M.S., & Cahalan, J.H., 1992. A preliminary evaluation of wave attenuation by four species of seagrass. Estuarine, Coastal and Shelf Science, 35(6), pp. 565-576.

Gastescu, P., 1983. The Danube Delta: Geographical characteristics and ecological recovery. *GeoJurnal*, 29,1, 57-67.

Giosan, L. et al., 1999. Longshore Sediment Transport Pattern along the Romanian Danube Delta Coast. Journal of Coastal Research, 15 (4), pp. 859-871.

Grases, A., 2017. Flooding and erosion assessment at Riumar (Ebro Delta). Master thesis, Universitat Politècnica de Catalunya.

Halcrow UK et al., 2011-2012. Master Plan 'Protection and Rehabilitation of the coastal zone'.

Halcrow Romania, 2011. Wave Modelling Report. Reduction of Coastal Erosion on the Black Sea Coast.

Hasselmann, K. et al., 1973. Measurements of wind-wave growth and swell decay during the Joint North Sea Wave Project (JONSWAP). Ergänzungsheft 8-12, pp. 73-74.

Holthuijsen, L.H., 2007. Waves in Oceanic and Coastal Waters. New York, NY: Cambridge University Press.

JICA (Japan International Cooperation Agency), 2007. Executive Summary. Basic Study and Coastal Protection Plan.

JICA (Japan International Cooperation Agency), 2008. Final Report. The Study on Protection and Rehabilitation of the Southern Romanian Black Sea Shore. in Romania

Kirwan, M. L. & Megonigal, J. P., 2013. Tidal wetland stability in the face of human impacts and sea-level rise. Nature 504, 53–60.

Kobayashi, N., Raichle, A.W. and Asano, T., 1993. Wave ateniuation by vegetation. Journnal of waterway, Port, Coastal and Ocean Engineering, 119(1), pp. 30-48.

Koftis, T., Prinos, P. and Stratigaki, V., 2013. Wave damping over artificial Posidonia oceania meadow: a large-scale experimental study. Coastal engineering 73(1), pp. 71-83.

Lesser, G.R. et al., 2004. Development and validation of a three-dimensional morphological model. Coastal Engineering, 51(8-9), pp. 883-915.

Lin-Ye, J. et al., 2018. Multivariate Hybrid Modelling of Future Wave-storms at the Northwestern Black Sea. Water 2018, 10(2), 221.

Manca, E. et al., 2012. Wave energy and wave-induced flow reduction by full-scale model Posidonia oceania seagrass. Continental Shelf Research, 50-51(1), pp. 100-116.

Mari-Isabella, 2014. The influence of coastal erosion on the development of southern Romanian Black Sea coastline. JIDEG, (9), 53-56.

Marin, O., Abaza, V. and Sava, D., 2013. Phytobenthos - Key Biological element in Shallow marine waters. Cercetări Marine, 43, pp. 197-218.

Masselink, G. & Pattiaratchi, C.B., 2001. Seasonal changes in beach morphology along the sheltered coastline of Perth, Western Australia. Marine Geology, 172(3-4), pp. 243-263.

Möller, I. et al., 1999. Wave Transformation Over Salt Marshes: A Field and Numerical Modelling Study from North Norfolk, England. Estuarine, Coastal and Shelf Science, 49(3), pp. 411-426.

Möller, I. et al., 2006. Quantifying saltmarsh vegetation and its effect on wave height dissipation: Results from a UK east coast saltmarsh. Estuarine, Cosatal and Shelf Science, 69(3-4), pp. 337-351.

Möller, I. et al., 2014. Wave attenuation over coastal salt marshes under storm surge conditions. Nature Geoscience, 7(10), pp. 727-731.

Myrhaug, D. & Holmedal, L.E., 2011. Drag force on a vegetation field due to long-crested and short-crested nonlinear random waves. Coastal Engineering, 58, pp. 562–566.

Narayan, S. et al., 2016. The Effectiveness, Costs and Coastal Protection Benefits of Natural and Nature-Based Defences. PLoS ONE 11(5), e0154735.

Nenciu, C. & Coman., C., 1996. Coastal processes and issues, specific in Romania. Proceedings of the International Workshop, pp. 309-313.

Nita, V., Micu, D. & Nenciu, M., 2014. First attempt of transplanting the key-species Cystoseira barbata and Zostera noltei at the Romanian coast. Cercetari Marine, 44, pp. 147-163.

Ondiviela, B. et al., 2014. The role of seagrasses in coastal protection in a changing climate. Coastal Engineering, 87, pp. 157-168.

Onea, F., & Rusu, L., 2017. A long-term assessment of the Black Sea wave climate. Sustainability, 9(10), 1875.

Panin, N., 1996. Impact of global changes on geo-environmental and coastal zone state of the Black Sea. Geo-Eco-Marina, 1, pp. 7-23.

Panin, N., 1998. Danube Delta: Geology, Sedimentology, Evolution. Association des Sédimentologistes Français, pp. 65.

Pons, L.G., Morphology, climate, geology and soils, 1992. *Conservation Status of the Danube Delta, Environmental Status Report 4*. Cambridge, UK, IUCN, 107p.

Pontee, N. et al., 2016. Nature-based solutions: lessons from around the world. Proceedings of the Institution of Civil Engineers: Maritime Engineering, 169(MA1), pp. 29-36.

Postolache, I. et al., 1995. Geomorphological and physical aspects of the Romanian Coast; Assessment of coastal change, Proceedings of Conference on Coastal Change, pp. 511-517.

Short, F.T. et al., 2010. Zostera noltii. The IUCN Red List of Threatened Species 2010: e.T173361A6999224.

Sierra, J.P. et al., 2017. Green measures for Mediterranean harbours under a changing climate. Proceedings of the Institution of Civil Engineers - Maritime Engineering, 170(2), pp. 55-66.

Suzuki, T. et al., 2012. Wave dissipation by vegetation with layer schematization in SWAN. Coastal Engineering, 59, pp. 64-71.

Surigui, C. & Razvan, M., 2013. Is the Tourism Sector Supportive of Economic Growth? Empirical Evidence on Romanian Tourism. Tourism Economics, 19(1).

The SWAN Team, 2018. Scientific and technical documentation. SWAN Cycle III version 41.20A. Delft University of Technology.

Verduin, J.J. & Backhaus, J.O., 2000. Dynamics of plant-flow interactions for seagrass Amphibiolis antarctica: field observations and model simulations. Estuarine, Coastal and Shelf Science, 50(2), pp. 185-204.

Acknowledgements

The present thesis represents the culmination of four years of university studies, throughout which I have had the opportunity to grow personally and professionally as a Civil Engineer.

I would like to thank the support received from my supervisors, Vicenç Gracia García, Manuel García-León and Irina Dinu; this thesis would not have been possible without their invaluable help. In addition, I want to thank Jue Lin-Ye for her help with the wave climate data.

Also, I would like to specially thank Irina for giving me the opportunity to visit GeoEcoMar in Bucharest, and her hospitality and help through all my days there.

Moreover, I am profoundly indebted for the patience and encouragement shown by my family and friends.

Finally, I assume the responsibility for the errors that may exist in this thesis and I apologize to you, the reader, for them. Thanks for your willingness to go through the text.

Monclús i Bori, Albert